Wavelets and Turbulence

MARIE FARGE, NICHOLAS KEVLAHAN, VALÉRIE PERRIER, AND ÉRIC GOIRAND

Invited Paper

We have used wavelet transform techniques to analyze, model, and compute turbulent flows. The theory and open questions encountered in turbulence are presented. The wavelet-based techniques that we have applied to turbulence problems are explained and the main results obtained are summarized.

I. Introduction

We first planned to write an up-to-date review of the use of wavelets and related multiscale techniques in turbulence to update previous reviews we have written on this topic [58], [59], [65]. To prepare this review we collected all the relevant papers we know of and discovered that there are more than 150. We then realized that our first goal of writing an exhaustive review was not realistic. We have decided instead to focus on the main applications of wavelets and wavelet packets to analyze, model, and compute turbulent flows.

We thank everyone who has helped us to gather this large set of papers on the applications of wavelets to the study of turbulence. We have listed them in a thematic bibliography, which is available via anonymous ftp (to ftp.lmd.ens.fr in the directory MFGA/pub/wavelets). The papers we will discuss here represent a small subset of this bibliography and they are for the most part directly related to our own research on 2-D turbulence. We apologise for this lack of objectivity, but we felt that it would be more realistic (in the limited number of pages we have) to focus on the problems we know best.

Our paper is organized as follows. We first state the problem of turbulence and the main open questions. We then focus on how wavelets and wavelet packets can be used to answer these questions. We present fractal and multifractal analysis, turbulence analysis and turbulence modeling, and finally the use of wavelets to numerically solve various partial differential equations related to turbulence. In conclusion, we present several perspectives and point out where new methods need to be developed in order to improve our understanding of turbulence.

Manuscript received June 1, 1995; revised December 15, 1995. This work was supported in part by the NATO Collaborative Research on Wavelet Methods in Computational Turbulence under Contract CRG-930456 and in part by the CEE Human Capital and Mobility program on 2-D Turbulence, Vortices and Geophysical Flows under Contract ERB-CHRX-CT92-0001.

M. Farge, N. Kevlahan, and V. Perrier are with the Laboratoire de Météorologie Dynamique du CNRS, Ecole Normale Supérieure, 75231 Paris Cedex 5, France.

E. Goirand is with ONERA, 92320 Châtillon-sous-Bagneux, France.

Publisher Item Identifier S 0018-9219(96)02573-X.

II. Open Questions in Turbulence

A. Definitions

Turbulence is a highly unstable state of fluids, where by fluids we mean continuous movable and deformable media. Liquids, gases, and plasmas are considered to be fluids when the scale of observation is much larger than the molecular mean free path. Turbulence is characterized by the Reynolds number, which is the ratio of the nonlinear convective motions, responsible for the flow instability, to the linear dissipative damping, which converts kinetic energy into thermal energy. We will focus on "fully developed turbulence," namely the limit of very large Reynolds numbers, which corresponds to either very large velocities (strong convection), and/or very small viscosity (weak dissipation), and/or very large turbulent scales. For flows encountered in hydraulics and naval engineering Reynolds numbers are of the order of 10^2 to 10^6, in aeronautics (engines, airplanes, shuttles) 10^6 to 10^8, in meteorology and oceanography 10^8 to 10^{12}, and in astrophysics larger than 10^{12}.

While the dissipation term is optimally represented in Fourier space because Fourier modes diagonalize the Laplacian operator (for periodic boundary conditions), the nonlinear convective term is very complicated in Fourier space where it becomes a convolution, i.e., all Fourier modes are involved. By the very simple argument that fully developed turbulence corresponds to flows where nonlinear convection is dominant, i.e., is larger than linear dissipation by a factor of the order of Reynolds number, it is obvious that the Fourier representation is inadequate for studying and computing flows in this large Reynolds limit. We need to find a mathematical tool to optimally solve the nonlinear convection term, in the same way as the Fourier transform is the most economical representation to solve the linear dissipation term. Surprisingly, however, all classical methods in turbulence rely on the Fourier representation,

which is inappropriate for the nonlinear convection term. See [125] for the statistical theory of 3-D turbulence and [98] for the statistical theory of 2-D turbulence.

Turbulence remains an unsolved problem because our present conceptual and technical tools are inadequate. For instance, Hamiltonian mechanics describes equilibrium states of conservative systems, but turbulent flows are nonstationary and dissipative. Classical dynamics only solves systems with a few degrees of freedom, while fully developed turbulent flows have a very large, perhaps even infinite, number of degrees of freedom. Statistical theories deal with closed reversible systems in thermal equilibrium, but turbulent flows are open irreversible systems out of thermal equilibrium. Mathematical methods solve linear differential equations, but cannot (apart from a very few cases) integrate analytically the nonlinear partial differential equations encountered in the study of turbulence. They are even unable to prove existence and uniqueness of solutions of the Navier–Stokes equations describing the fluid motions when nonlinear advection becomes dominant. We should mention here a recent mathematical result [31] which gives, using multiscale (Paley–Littlewood) decomposition, a local existence and uniqueness theorem for Navier–Stokes equations in R^3 if initial conditions are sufficiently oscillating (in a Besov norm sense). Some other mathematical attempts have been made using divergence free vector wavelets [67], [17], but in all cases these proofs are done in an unbounded space. However, physical fluid flows are bounded either internally or externally, and we still do not know the optimal functional space for describing turbulent flows.

In summary, the theory of fully developed turbulence is in what we call a prescientific phase, because we do not yet have an equation, nor a set of equations, that could be used to efficiently compute turbulent flows. The incompressible Navier–Stokes equations, which are the fundamental equations of fluid mechanics, are not the right ones for turbulence because their computational complexity becomes intractable for large Reynolds flows. However, in this limit it should then be possible, as it is done in statistical mechanics, to define averaged quantities which would be the appropriate variables to describe turbulence and then find the corresponding transport equations to compute the evolution of these new quantities. Likewise, the Navier–Stokes equations can be derived from the Boltzmann equation by considering appropriate limits (Knudsen and Mach numbers tending to zero [9], [10]) and appropriate averaging procedures to define new coarse-grained variables (velocity and pressure) and associated transport coefficients (viscosity and density). The turbulence equations should be derived as a further step in this hierarchy of embedded approximations, but this scientific program may be impaired by the possible nonuniversality of turbulence, which remains an essential question to address.

More precisely, it is easier to define the appropriate parameters to go from Boltzmann to Navier–Stokes than from Navier–Stokes to turbulence equations [122]. In the first case only a linear averaging procedure, namely coarse-graining, is needed while in the second case we have to find an appropriate nonlinear procedure, namely some conditional averaging. For this we should first identify the dynamically active structures constituting turbulent flows, classify their elementary interactions, and define the averaging procedures to construct appropriate statistical observables. Wavelet analysis is a good tool for exploring this conditional averaging and for seeking an atomic decomposition of phase space, defined in both space and scale. In 1972, Tennekes and Lumley [151] already had the intuition of such a phase-space decomposition when they proposed to consider a turbulent flow as a superposition of Gaussian-shaped wave packets they called eddies; but we know since Balian's theorem [8] that we cannot built orthogonal bases with such functions. This is why we propose to use instead wavelet or wavelet packet bases to study how phase-space "atoms" exchange energy, or other important dynamical quantity, during the flow evolution and possibly combine to form phase-space "molecules."

We still hope that there will be enough universality in the behavior of these phase-space "atoms" so that we can find a general theory and a set of equations to describe their evolution, but this could well be an unrealistic goal. Wavelets may supply new functional bases better adapted to represent and compute turbulent flows, i.e., to extract their elementary dynamical entities, perform the appropriate averages on them, and predict the evolution of these statistical quantities.

B. Navier–Stokes Equations

The fundamental equations of the dynamics of an incompressible (constant density of fluid elements) and Newtonian (deformation proportional to velocity gradients) fluid are the Navier–Stokes equations

$$\partial_t \mathbf{V} + (\mathbf{V} \cdot \nabla)\mathbf{V} + 1/\rho \nabla P = \nu \nabla^2 \mathbf{V} + \mathbf{F} \tag{1}$$

$$\nabla \cdot \mathbf{V} = 0 \tag{2}$$

$$\text{plus initial and boundary conditions} \tag{3}$$

where t is the time, $\mathbf{V}$ the velocity, P the pressure, $\mathbf{F}$ the resultant of the external forces per unit of mass, ρ a constant density, and ν a constant kinematic viscosity.

The mathematical difficulty of the Navier–Stokes equations arises from the fact that the small parameter ν, which tends to zero in the limit of infinite Reynolds numbers, i.e., for fully developed turbulent flows, appears in the term containing the highest-order derivative, namely the dissipation term $\nu \nabla^2 \mathbf{V}$. Thus the character of the equations changes as ν tends to zero, since in this limit it is the nonlinear advection term $(\mathbf{V} \cdot \nabla)\mathbf{V}$ which dominates. This singular limit is similar to the semiclassical limit $\hbar \to 0$ encountered in quantum mechanics. When $\nu = 0$, i.e., for infinite Reynolds numbers, the Navier–Stokes equations are called Euler's equations.

The physical difficulty of the Navier–Stokes equations comes from the incompressibility condition, namely the

divergence-free requirement imposed by (2), which implies that the speed of sound is infinite. In this case any local perturbation is instantaneously transmitted throughout the whole domain. This requirement seems too drastic and quite unphysical because the speed of sound is large in real flows but never infinite. In the future we may prefer to consider instead weakly compressible Navier–Stokes equations to simplify the computation of turbulent flows and represent their local behavior more accurately. Moreover, on physical grounds Euler's equations are unrealistic because the limit $\nu = 0$ contradicts the fluid hypothesis, which supposes that the system is locally close to thermodynamical equilibrium due to molecular collisions (which implies dissipation).

The pressure can be eliminated by taking the curl of (1) and (2). This gives the equation of vorticity ω, the curl of velocity

$$\partial_t \omega + (\mathbf{V} \cdot \nabla)\omega = (\omega \cdot \nabla)\mathbf{V} + \nu \nabla^2 \omega + \nabla \times \mathbf{F}. \quad (4)$$

If one considers a stationary state of the turbulent flow such that all the energy (integral of the velocity squared) and enstrophy (integral of the vorticity squared) injected into the flow by the external forces are dissipated by viscous friction, (4) becomes

$$d_t \omega = (\omega \cdot \nabla)\mathbf{V}. \quad (5)$$

In 3-D this equation shows that vortex tubes may be stretched by velocity gradients, a mechanism which has been proposed to explain the transfer of energy toward the smallest scales of the flow. In 2-D the right-hand side becomes zero, because the vorticity is then a pseudo-scalar $\omega = (0, 0, \omega)$ perpendicular to the velocity gradients. The vorticity and its infinitely many moments are therefore Lagrangian invariants of the flow (Helmholtz theorem). In this case there is no vortex stretching and energy cannot cascade toward the smallest scales, but tends to accumulate into the largest scales, the so called inverse energy cascade [97], [13], while enstrophy instead cascades toward the smallest scales where it accumulates.

C. Statistical Theories of Turbulence

The first statistical method was proposed in 1894 by Reynolds [139] who assumed that turbulent flows can be described by ensemble averages, without considering the details of each flow realization. He then decomposed the velocity field $\mathbf{V}(\mathbf{x})$ into a mean contribution $\bar{u}_i$ plus fluctuations u_i' and rewrote the Navier–Stokes equations to predict the evolution of $\bar{u}_i$, which gives the Reynolds equations

$$\frac{\partial \bar{u}_i}{\partial t} + \bar{u}_j \frac{\partial \bar{u}_i}{\partial x_j} + \frac{1}{\rho}\frac{\partial \bar{P}}{\partial x_i} = \frac{\partial}{\partial x_j}\left(\nu \frac{\partial \bar{u}_i}{\partial x_j} - \overline{u_i' u_j'}\right) + \bar{F}_i. \quad (6)$$

To solve the Reynolds equations one should compute the second order moment of the velocity fluctuations $\overline{u_i' u_j'}$, called the Reynolds stress tensor, which in fact depends on the third order moment $\overline{u_i' u_j' u_k'}$ (i, j, and k are dummy indexes), which depends on the fourth order moment, and so on *ad infinitum*. This is the closure problem: there are more unknowns than equations; to solve the hierarchy of Reynolds equations the traditional strategy is to introduce another equation, or system of equations, chosen from some *a priori* phenomenological hypotheses, to close the set of Reynolds equations.

For instance, to close the hierarchy of Reynolds equations, Prandtl introduced a characteristic scale for the velocity fluctuations, called the mixing length, which led him to rewrite the Reynolds stress tensor as a turbulent diffusion term. Following an hypothesis proposed by Boussinesq [26], and by analogy with molecular diffusion which smooths velocity gradients for scales smaller than the molecular mean free path, Prandtl assumed that there exists a turbulent diffusion which regularizes the mean velocity gradients for scales smaller than the mixing length. Unfortunately this hypothesis is wrong because, contrary to molecular diffusion, which is decoupled from the large scale motions and can then be modeled by a linear operator (Laplacian) with an appropriate transport coefficient (viscosity), turbulent motions interact nonlinearly at all scales and there is no spectral gap to decouple large scale motions from small scale motions. This is a major obstacle faced by all turbulence models and the closure problem remains open. This is also the reason why renormalization group techniques [161] and nonlinear Galerkin numerical methods [117] have not met their promises. An important direction of research is to find a new representation of turbulent flows in which there is a gap, decoupling motions out of equilibrium from well thermalized motions, which can then be modeled. Such a separation seems only possible with a nonlinear closure, based on conditional averages which depend on the local behavior of each flow realization. Nonlinear wavelet or wavelet packet filters are good candidates for this (see Section V-B).

Taylor [150], under the influence of Wiener with whom he was in correspondence [16] since his famous paper on turbulent diffusion [169], proposed in 1935 characterizing turbulent fields by their correlation functions, in particular by the Fourier transform of their two-point correlation function which gives their energy spectrum. Twenty years before, Einstein [51] had outlined the same method to characterize fluctuating data, but he was not followed at the time [160]. To simplify the computation of correlation functions, Taylor made the hypothesis of statistical homogeneity and isotropy of turbulent flows, supposing that the ensemble averages are invariant under both translation and rotation. In the thirties Gebelein proposed applying the probability theory of Kolmogorov to hydrodynamics, a method later developed by Kolmogorov himself and his student Obukhov [127], who published in 1941 three key papers on the statistical theory of fully developed turbulence. Kolmogorov [93]–[95] studied the way in which Navier–Stokes equations in 3-D distribute energy among the different scales of the flow. This type of approach is common in statistical mechanics, but a difficulty arises here from the fact that turbulent flows are open thermodynamical systems, due to the injection of energy by external forces and its dissipation by viscous frictional forces. To resolve

this difficulty Kolmogorov supposed that external forces act only on the largest scales while frictional forces act only on the smallest scales, which, in the limit of very large Reynolds numbers, leaves an intermediate range of scales, called the inertial range, in which energy is conserved and only transferred from large to small scales at a constant rate ϵ which is supposed to be constant. But this cascade of energy concerns averages and not individual flow realizations; moveover it is only phenomenological and has never been proved from first principles. Kolmogorov also supposed that turbulent flows are statistically homogeneous and isotropic; he also uses the fact that the skewness, namely the departure from Gaussianity of the velocity increment probability distribution, is constant, which implies that the flow is non intermittent. These hypotheses lead him to the K41 model which predicts the following energy spectrum scaling, known as the $k^{-5/3}$ law

$$E(k) = C\epsilon^{2/3}k^{-5/3} \tag{7}$$

where k is the modulus of the wavenumber averaged over directions, corresponding to the inverse of the scale, and C is called Kolmogorov's constant.

Landau criticized Kolmogorov's hypothesis of a constant rate of energy transfer ϵ independent of the scale, arguing that the dissipation field should also be considered random. Following this remark Kolmogorov proposed to model the energy transfer as a multiplicative process where only a fraction β of energy is transferred from one scale to another. Assuming that the probability density of the dissipation field varies randomly in space and time with a log-normal law, this lead him to propose the K62 model which predicts the following energy spectrum scaling

$$E(k) = C\epsilon^{\frac{2}{3}}k^{-\frac{5}{3}}\ln\left(\frac{k}{k_I}\right)^{\beta} \tag{8}$$

where k_I is the wavenumber at which energy is injected (inverse of the integral length scale).

For 2-D turbulence there is a statistical theory similar to Kolmogorov's theory developed by Batchelor [13] and Kraichnan [93] which takes into account, in addition to the conservation of energy, the conservation of enstrophy (integral of vorticity squared), true only for the 2-D Euler equations. Making the same kind of hypotheses as Kolmogorov, they predicted a direct enstrophy cascade, from large to small scales, giving a k^{-3} energy spectrum, and an inverse energy cascade, from small to large scales, giving a $k^{-5/3}$ energy spectrum. The problem is that the energy spectra obtained from numerical simulations are always steeper than the k^{-3} law predicted by this theory. There is another more recent statistical theory proposed by Polyakov [136] which takes into account, in addition to the energy conservation, the conservation of infinitely many moments of vorticity in 2-D, which led him to predict different scalings depending on the way energy is injected; thus, Polyakov's theory is not universal. In fact the same nonuniversal behavior of 2-D turbulence is also observed in numerical simulations [103].

Since the pioneering work of Onsager [129], there have been several statistical theories for decaying 2-D turbulence [90], [143], [120], [144], [44], [145], [56] which are not based on ensemble averages nor spectral information. These theories, unlike those of Kraichnan's and Polyakov's, do not discard the spatial flow structure. For a recent review of these theories a good reference is [116]. Onsager's theory assumes that all vorticity is concentrated into a finite number of point vortices and predicts that there exist negative temperature states; more precisely it predicts that high energy states can be favored compared to low energy states, contrary to classical statistical physics. These negative temperature states correspond to the clustering of same-sign vortices characteristic of the inverse energy cascade of 2-D turbulence. But the extension of Onsager's approach to describe continuous vorticity fields, involving infinite number of degrees of freedom, leads to a highly singular limit which has been overcome only recently using large deviation probabilities and maximum entropy techniques. This new theory, due independently to Robert [144], [145] and Miller [120], predicts final stationary states (in the absence of external forces) characterized by a functional relation between coarse-grained vorticity and stream function. This relation is called the coherence function and it seems to be verified for strong mixing situations, such as 2-D shear layers or vortex merging [148].

D. Coherent Structures

Since the beginning of turbulence research there has been, alongside the statistical approach based on ensemble averages, a tendency to analyze each flow realization separately. This leads to the recognition that turbulence contains coherent structures, even at very large Reynolds [89]. Examples of coherent structures include the Karman vortices observed by Roshko in 1961 at a Reynolds number of 10^7 [146], the horseshoe vortices observed in turbulent boundary layers and mixing layers [34], and the vorticity tubes (often called filaments) [39], [28] observed in statistically homogeneous flows. Coherent structures are defined as local condensations of the vorticity field which survive for times much longer than the eddy turnover time characteristic of the energy transfers.

The vorticity field is easy to visualize in numerical experiments, but very difficult to visualize in laboratory experiments; therefore, one usually observes the pressure field instead. Indeed, if we take the divergence of (1) we obtain

$$2\nabla^2 P/\rho + \sigma^2 - \omega^2 = \nabla \cdot \mathbf{F} \tag{9}$$

where $\sigma = \frac{1}{2}(\partial_i u_j + \partial_j u_i)$ is the rate of strain which controls dissipation. This equation shows that vorticity concentrations corresponding to coherent structures are sources of low pressure, while strained regions corresponding to dissipation, are sources of high pressure. Couder *et al.* [39], [28] recently measured the histogram of the probability distribution function of pressure and showed that for the large negative pressures it has an exponential behavior, while for the pressures around zero it has a Gaussian

behavior. In other words, the coherent structures, which are characterized by strong depressions, are responsible for the non-Gaussian behavior of turbulent flows, which confirms a similar conclusion drawn before by Van Atta and Antonia [154] from measurements of the spatial gradients of velocity. This has also been shown by Abry *et al.* [2] using wavelet techniques to separate the coherent structures from the background flow in a 1-D cut of pressure signal.

The mere existence of coherent structures invalidates the ergodic hypothesis, which is an essential ingredient of any statistical theory, and which also justifies the Taylor hypothesis widely used in turbulence analysis. According to the Taylor hypothesis, ensemble averages can be replaced by time or space averages, which are easier to obtain in both laboratory and numerical experiments. As far as we know, all existing experimental results measuring the turbulence energy spectrum rely on the Taylor hypothesis and we are therefore sceptical of their validity as long as the flow is intermittent. Concerning numerical experiments, we interpret the energy spectrum and its inertial range power-law form as characteristic of the random processes responsible for turbulence. In practice, however, we analyze only one flow realization because in most simulations the correlation length is the size of the computational periodic domain. In this case, a power-law behavior should be interpreted as indicating the presence of some quasi-singular structures in the flow, and not as a proof of its random dynamics. This new point of view led Saffman [171] to interpret the energy power-law behavior as resulting from the presence of vorticity fronts; later Farge and Holschneider [64] proposed another interpretation based on the emergence of cusp-like coherent structures, which correspond to the limit case of negative temperature states [30]. The wavelet transform, because it measures the local scaling of a field, is the appropriate tool for verifying these different interpretations in relating the power-law scaling of the energy spectrum to the geometry of coherent structures.

Today we still do not have a complete theory to explain the formation and persistence of coherent structures, and we shall have to be content with a qualitative description of their behavior. This is more evidence that we are still in a prescientific phase, having as yet only a limited grasp of the nature of turbulence. The new point of view is to consider that coherent structures are generic to turbulent flows, even at very high Reynolds numbers, and that they probably play an essential role in their intermittency. Indeed, several wind tunnel experiments [15], [3] have shown that the energy associated with the smallest scales of turbulent flows is not distributed densely in space and time. This has led various authors to conjecture that the support of the set on which dissipation occurs should be fractal [115], [73], or multifractal [130]. It is now thought [63], but not proven, that the time and space intermittency of turbulent flows is related to the presence of coherent structures. This is still an open question and wavelet analysis seems to be the appropriate technique to answer it.

The classical theory of turbulence is blind to the presence of coherent structures because they are advected by the flow in a homogeneous and isotropic random fashion, and hence they are lost by ensemble averaging. Moreover, the spatial support of coherent structures becomes smaller and smaller when Reynolds number increases, whereas in 3-D flows coherent structures (vorticity tubes often called filaments) become highly unstable [39] and therefore their temporal and spatial support may be very small. Consequently, the presence of coherent structures only affects the high-order velocity structure functions (defined as the high-order statistical moments of the velocity increments) which are most sensitive to unusual or extreme events (large deviations). The high-order structure functions have been measured only recently [3], because their calculation requires very long data sequences. They do not follow Kolmogorov's theory which predicts a linear dependence of the scaling exponent of the velocity structure functions on their order. Van der Water [156] has observed that there are in fact two distinct nonlinear dependencies for odd and for even orders, which may be interpreted in terms of the multispiral model of Vassilicos [155].

In conclusion, we can say that the presence of coherent structures is responsible for the non-Gaussian statistics of fully developed turbulent flows, which contradicts the Gaussian hypothesis made by Kolmogorov. Due to the sensitivity to initial conditions of turbulent flows, any theory of turbulence should be statistical. But before being able to construct a new statistical theory of turbulence, we need to find new types of averages able to preserve the information associated with coherent structures and therefore take into account the intermittency of turbulent flows. Wavelets can play a role there in separating the coherent (non-Gaussian) components from the incoherent (Gaussian) components of turbulent flows, in order to devise new conditional averages to replace the classical ensemble averages.

III. Fractals and Singularities

A. Introduction

According to the K41 model turbulence in the inertial range has a power law energy spectrum (7), and thus does not have a characteristic length scale. Therefore turbulence in this range of length scales looks similar at any magnification and can be described as self-similar. According to experimental observations, however, turbulence is also characterized by quasi-singular structures such as vortices and is intermittent (quantities such as energy dissipation vary greatly in time and space). A quasi-singular structure is one that appears singular until the dissipation scale at which the smoothing effect of viscosity becomes important.[2] In fact the theoretical $k^{-\frac{5}{3}}$ inertial range energy spectrum predicted by Kolmogorov's theory implies that some sort of quasi-singular distribution of velocity and vorticity must be present in turbulent flows [85], [121], [80].

[2]Note that for simplicity we shall use the terms "singular" instead of "quasi-singular" and "infinite" instead of "very large" throughout this section.

It remains an open question whether this quasi-singular behavior is due to the randomness of turbulent motions resulting from their chaotic dynamics or to the presence of localized quasi-singular structures resulting from an internal organization of the turbulent motions. Kolmogorov's theory is based on ensemble averages, but in using them we are unable to disentangle these two hypotheses. Ensemble averages should be replaced by an analysis of turbulence for each realization and be based on the local measurement and statistics of singularities for which we need effective ways of detecting and characterizing quasisingularities in turblent signals.

The *types* of singularities seen in turbulence may be divided into two classes: *cusps* (i.e., nonoscillating singularities in which the function or one of its derivatives becomes infinite at a certain point, e.g., $1/x$) and *spirals* (i.e., oscillating singularities in which the frequency of oscillation becomes infinite at a certain point, e.g., $\sin(1/x)$). Fig. 6 shows an example of a 2-D flow containing both a cusp (b) and a spiral (d). (A cut through the spiral is an oscillating singularity over a certain range of length scales.) Likewise the *distribution* of singularities in turbulence may also be divided into two classes: *isolated* (singularities at a finite number of points) and *dense* (singularities at an infinite number of points). Dense distributions of singularities are called fractals and are characterized by one (monofractal) or more (multifractal) fractal dimensions. Fig. 1(a) shows a typical fractal signal. Note that fractals may contain both cusp and spiral type singularities. Turbulence might contain both fractal and isolated distributions of singularities, and spiral and cusp types of singularities. Fig. 1(b) shows a spiral type singularity with fractal noise superimposed; both the noise and the spiral have the same energy spectrum.

This section is concerned with wavelet-based techniques for calculating quantities such as energy spectra, structure functions, singularity spectra and fractal dimensions. These subjects are connected by the fact that they all measure the local regularity of the signal (i.e., strength of singularities in the signal). For example, the slope of the usual Fourier energy spectrum of a signal containing only isolated cusp singularities is determined by the strongest singularity [164]. The advantage of the wavelet transform is that it is able to analyze locally the singular behavior of a signal. One can then use this local information to construct statistics describing the distribution and type of singularities (e.g., multifractals), or define local or conditionally averaged versions of traditional measures such as the energy spectrum and structure functions. We are primarily concerned with cusp type singularities (either isolated or fractal), although we also discuss methods for distinguishing between signals containing isolated spirals and purely fractal signals.

In Section III-B we review the mathematical results on one of the key properties of wavelet transforms: their ability to detect and characterize singular structures. We then describe three related applications which rely on this property: calculation of local energy spectra, structure functions (Section III-C) and the singularity spectra which characterize multifractals (Section III-E). These wavelet methods generally require the assumption that the singularities of the signal are cusps. Because isolated spirals are likely to be present in turbulence it is essential to have a method of determining which sort of singularity a signal contains. In Section III-F we review a different wavelet-based method for distinguishing between signals containing isolated spirals and purely fractal signals (the two types of signal most likely to be measured in a turbulent flow). Each section gives a practical review of the method and briefly summarizes some results that have been obtained for turbulence data. Formulating these techniques in terms of wavelet transforms brings out the connections between them as well as providing new information, and this point is emphasized throughout this section.

B. Detection and Characterization of Singularities

The most useful property of the wavelet transform is its ability to detect and accurately measure the strength (given by the Hölder exponent) of individual singularities in a signal. A function $f(x)$ has a Hölder exponent $\alpha(x_0)$ and is called $C^{\alpha}(x_0)$ if

$$|f(x) - f(x_0)| \leq C|x - x_0|^{\alpha(x_0)} \quad \text{as } x \to x_0. \tag{10}$$

Note that (10) can hold for large α even if f is not differentiable near x_0. The exponent $\alpha(x_0)$ therefore measures the smoothness of the function $f(x)$ near x_0: the larger $\alpha(x_0)$ is, the smoother or more regular the function $f(x)$ is near x_0 while the smaller $\alpha(x_0)$ is, the rougher or more singular the function is. If the Hölder exponent is negative there is an actual singularity of the function at x_0 (or a quasisingular behavior near x_0 over a certain range of length scales if one is measuring a physical quantity like velocity). A function f is C^{α} if (10) is true with the same C for any x_0.

It is important to note that (10) does not hold for oscillating singularities because in this case the Hölder exponent increases by more than one when the function is integrated. This anomalous behavior is due to the fact that there are an infinite number of accumulating oscillations in the neighborhood of the singularity.

Consider the L^1 norm wavelet transform (which conserves the L^1 norm of a function)

$$\tilde{f}(x,r) = \frac{1}{r}\int_{-\infty}^{\infty} f(x')\psi\left(\frac{x'-x}{r}\right)dx'. \tag{11}$$

The wavelet transform is thus a 2-D function in position x and scale r. Mallat and Hwang [114] have shown that singularities in $f(x)$ produce a maximum in the modulus of the wavelet transform $|\tilde{f}(x,r)|$ and that following the position of a wavelet modulus maximum as $r \to 0$ gives the position x_0 of the singularity. Furthermore, each singularity has an associated "influence cone defined by

$$|x - x_0| \leq Cr \tag{12}$$

and if the singularity is an isolated cusp then the wavelet transform modulus for all points within the influence cone is

$$|\tilde{f}(x,r)| \leq Ar^{\alpha(x_0)} \tag{13}$$

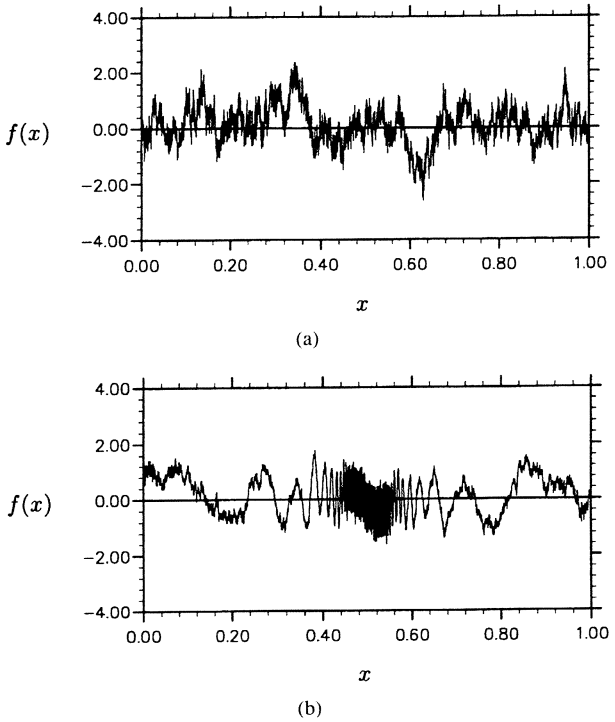

Fig. 1. Different types and combinations of singularities. (a) A fractal signal with energy spectrum $E(k) \propto k^{-\frac{5}{3}}$. (b) A spiral with fractal noise (both noise and spiral have the same energy spectrum $E(k) \propto k^{-\frac{5}{3}}$).

provided that the at least the first $n > \alpha(x_0)$ moments of the analyzing wavelet $\psi(x)$ vanish, where the nth moment is defined by the integral

$$\int_{-\infty}^{+\infty} x^n \psi(x)\, dx. \tag{14}$$

Equation (13) shows that the Hölder regularity $\alpha(x_0)$ can be found from the slope of a straight line that remains above the graph of $\log|\tilde{f}(x,r)|$ versus $\log r$ at a position x satisfying inequality (12). When several singularities are present only the nonoverlapping parts of the cones associated with each singularity satisfy (13). Intuitively, it is the self-similar scaling property of the wavelet which allows the wavelet transform to measure the rate of self-similar narrowing with decreasing scale which characterizes the strength of a cusp singularity.

If the singularity is not isolated and there is only one zero crossing of the wavelet transform near x_0, one can find the regularity in the left and right neighborhoods of x_0 by measuring the decay of the wavelet modulus transform along maxima lines of the wavelet transform to the left and right of the influence cone of x_0.

In practice, such graphs of $\log|\tilde{f}(x,r)|$ versus $\log r$ contain oscillations superimposed on the power-law behavior which can make it difficult to determine the slope at larger scales. Vergassola and Frisch [157] showed that these oscillations are necessarily present for any self-similar random process whether or not the signal is multifractal (the lacunarity of multifractal signals should also produce oscillations). These oscillations can be reduced by finding the average decay of the wavelet modulus along many lines in the influence cone, or by averaging the decay along vertical lines at many different points (e.g., one may be interested in the conditionally averaged scaling of points in regions of irrotational straining). Arnéodo *et al.* [4] have suggested that the deviations from a strict power law may be reduced by measuring the decay of the modulus of the wavelet transform along the line of maximum modulus within the influence cone.

The analysis of signals containing spiral singularities either isolated (e.g., $\sin 1/|x - x_0|$) or fractal (e.g., the Riemann–Weierstrass function) is more complicated because the worst singular behavior of a spiral singularity appears below the cone of influence. In this case one measures the decay as $r \to 0$ of the modulus of the wavelet transform along the set of points which are general maxima below the cone of influence (i.e., maxima in both the position and scale directions). This gives an upper bound on the Hölder exponent, but in general one has to use lines of maximum modulus both inside and outside the cone of influence to fully determine the singular behavior of an oscillating singularity.

Arnéodo *et al.* [5] have recently carried out work defining two wavelet-based exponents that measure the strength of an oscillating singularity. They find that the faster the frequency increases, the more irregular its derivative. In general, oscillating behavior appears in fractal objects that are self-similar under nonhyperbolic mappings, e.g., the Riemann–Weierstrass function or the Farey-tree partitioning of rationals.

C. Energy Spectra

The Fourier energy spectrum has been one of the most popular techniques for turbulence analysis, indeed traditional turbulence theory was constructed in Fourier space [14]. The Fourier energy spectrum $E(k)$ of the real function $f(x)$ is defined by

$$E(k) = \frac{1}{2\pi}|\hat{f}(k)|^2 \quad \text{for } k \geq 0 \tag{15}$$

where $\hat{(\cdot)}$ signifies Fourier transform. In traditional turbulence theory the phase infomation is lost and only the modulus of the Fourier transform is used. This is probably a major weakness of the traditional way of analyzing turbulence since it neglects any organization of the turbulent velocity field.

The wavelet transform extends the concept of energy spectrum so that one can define a local energy spectrum $\tilde{E}(x,k)$ using the L^2 norm wavelet rather than the L^1 norm used in Section III-B (i.e., the wavelet transform is normalized by $1/r^{\frac{1}{2}}$ rather than by $1/r$)

$$\tilde{E}(x,k) = \frac{1}{2c_\psi k_0}\left|\tilde{f}\left(x, \frac{k_0}{k}\right)\right|^2 \quad \text{for } k \geq 0 \tag{16}$$

where k_0 is the peak wave number of the analyzing wavelet ψ and

$$c_\psi = \int_0^{+\infty} \frac{|\hat{\psi}(k)|^2}{k} dk. \tag{17}$$

By measuring $\tilde{E}(x,k)$ at different places in a turbulent flow one can determine what parts of the flow contribute most to the overall Fourier energy spectrum and how the energy spectrum depends on local flow conditions. For example, one can determine the type of energy spectrum contributed by coherent structures, such as isolated vortices, and the type of energy spectrum contributed by the unorganized part of the flow.

Since the wavelet transform analyzes the flow into wavelets rather than sine waves it is possible that the mean wavelet energy spectrum may not always have the same slope as the Fourier energy spectrum. Perrier *et al.* [132] have shown, however, that the mean wavelet spectrum $\tilde{E}(k)$

$$\tilde{E}(k) = \int_0^{+\infty} \tilde{E}(x,k) dx \tag{18}$$

gives the correct Fourier exponent for a power-law Fourier energy spectrum $E(k) \propto k^{-\beta}$ provided that the analyzing wavelet has at least $n > (\beta - 1)/2$ vanishing moments. This condition is obviously the same as that for detecting singularities derived in the previous section since $\beta = 1 + 2\alpha$ for isolated cusps. Thus, the steeper the energy spectrum the more vanishing moments of the wavelet we need. The inertial range in turbulence has a power-law form, as do the energy spectra of all self-similar processes. The ability to correctly characterize power-law energy spectra is therefore a very important property of the wavelet transform (which is of course related to its ability to detect and characterize singularities).

Note that if the singularities are all isolated cusps then the exponent of the Fourier energy spectrum is determined by the strongest singularity α of the signal

$$E(k) = Ck^{-2(\alpha+1)} \tag{19}$$

where C is a constant. If the singularities are spirals and/or are not isolated then the strongest singularity sets a lower bound on the exponent of the energy spectrum [157]

$$E(k) \leq Ck^{-2\alpha}. \tag{20}$$

The way the dense singularities accumulate can make the signal effectively more singular, decreasing the magnitude of the exponent of the energy spectrum by up to two. Because they are both controlled in the same way by singularities, the wavelet energy spectrum can be thought of as a sort of local Fourier transform.

The mean wavelet energy spectrum is a smoothed version of the Fourier energy spectrum. This can be seen from the following relation between the two spectra

$$\tilde{E}(k) = \frac{1}{c_\psi k} \int_0^{+\infty} E(\omega) \left| \hat{\psi}\left(\frac{k_0 \omega}{k} \right) \right|^2 d\omega \tag{21}$$

which shows that the mean wavelet spectrum is an average of the Fourier spectrum weighted by the square of the Fourier transform of the analyzing wavelet shifted at wavenumber k. Note that the larger k is, the larger the averaging interval. This property of the mean wavelet energy spectrum is particularly useful for turbulent flows. The Fourier energy spectrum of a single realization of a turbulent flow is too spiky to be useful, but one can measure a well-defined slope from the mean wavelet energy spectrum.

The Mexican hat wavelet

$$\hat{\psi}(k) = k^2 \exp(-k^2/2) \tag{22}$$

has only two vanishing moments and thus can correctly measure energy spectrum exponents up to $\beta < 5$. Only the zeroth order moment of the Morlet wavelet

$$\begin{aligned} \hat{\psi}(k) &= \tfrac{1}{2\pi} \exp(-(k - k_\psi)^2/2) \quad \text{for } k > 0 \\ \hat{\psi}(k) &= 0 \qquad\qquad\qquad\qquad\quad \text{for } k \leq 0 \end{aligned} \tag{23}$$

is zero, but the higher nth order moments are very small ($\propto k_\psi^n \exp(-k_\psi^2/2)$) provided that k_ψ is sufficiently large. Therefore the Morlet wavelet transform should give accurate estimates of the power-law exponent of the energy spectrum at least for approximately $\beta < 7$ (if $k_\psi = 6$).

Perrier and Basdevant [132] present a family of new wavelets with an infinite number of cancellations

$$\hat{\pi}_n(k) = \alpha_n \exp\left(-\frac{1}{2} \left(k^2 + \frac{1}{k^{2n}} \right) \right), \quad n \geq 1 \tag{24}$$

where α_n is chosen for normalization. The wavelets defined in (24) can therefore correctly measure any power-law energy spectrum. Furthermore, these wavelets can detect the difference between a power-law energy spectrum and a Gaussian energy spectrum ($E(k) \propto \exp(-(k/k_0)^2)$). It is important to be able to determine at what wavenumber the Gaussian energy spectrum begins since this wavenumber defines the end of the inertial range of turbulence and the beginning of the dissipative range.

One of the first measurements of local energy spectra in turbulence was reported by Meneveau [118]. Meneveau used the discrete wavelet transform to measure local energy spectra in experimental and direct numerical simulation (DNS) flows and found that the standard deviation of the local energy (a measure of the spatial fluctuation of energy) was approximately 100% throughout the inertial range. Meneveau also calculated the spatial fluctuation of $T(k)$ which measures the transfer of energy from all wavenumbers to wavenumber k. On average $T(k)$ is negative for the large scales and positive for the small scales, indicating that in 3-D turbulence energy is transferred from the large scales to the small scales where it is eventually dissipated (in agreement with Richardson's [141] cascade model of turbulence). Meneveau found, however, that at many places in the flow the energy cascade actually operates in the opposite direction, from small to large scales, indicating a local inverse energy cascade (also called backscattering). This local spectral information, which links the physical and Fourier space views of turbulence, can only be obtained using the wavelet transform.

D. Structure Functions

Another fundamental quantity in the classical theory of turbulence [89] is the pth order structure function $S_p(r)$

$$S_p(r) = \frac{1}{L}\int_0^L |f(x) - f(x+r)|^p dx \qquad (25)$$

where $L \gg r$ is the length of the signal, and L must be long enough so that $S_p(r)$ does not change if L is increased (and thus the increments of f should be stationary in x). The velocity signal of a turbulent flow varies in both space and time and between different realizations of the flow. Thus the integral in (25) should, in general, be replaced by a suitably defined ensemble average in order to calculate the structure function of turbulent velocities. To justify the use of space or time averages instead of ensemble averages (over different realizations of the flow) one supposes that the turbulent flow motions are ergodic, which is an unvalidated hypothesis and is probably wrong for 2-D turbulence. If the energy spectrum exponent β is in the range $1 < \beta < 3$ (as is usually the case for the inertial range of turbulence) the velocity increments are a stationary function even though the velocities themselves are not [41], this is a good reason to work with velocity increments rather than the velocities themselves since stationarity is necessary in order to justify estimating a quantity by averaging over space. The larger p the more $S_p(r)$ is dominated by extreme events. Thus the pth order structure function characterizes more and more extreme events as p increases.

If $f(x)$ is self-similar then, just as in the case of the energy spectrum, the structure functions will have a power law dependence on the scale r

$$S_p(r) = r^{\zeta(p)}. \qquad (26)$$

The first order structure function $\zeta(1)$ provides a measure of the smoothness of $f(x)$, and in fact $\zeta(1)$ is related to the box dimension D_F of the graph of $f(x)$

$$D_F = 2 - \zeta(1) \qquad (27)$$

where D_F measures the space-fillingness of $f(x)$. The second order structure function is related to the energy spectrum by

$$\beta = \zeta(2) + 1. \qquad (28)$$

The Kolmogorov theory [93] showed that the inertial range of turbulence has $\beta = 5/3$, or equivalently that

$$\zeta(p) = p/3 \qquad (29)$$

however, recent experiments [3] have shown that the structure function exponents increase more slowly than linearly with p for $p > 5$, contradicting Kolmogorov's theory. The cause of this difference is generally thought to be the fact that the energy dissipation $\varepsilon(x) = (du(x)/dx)^2$ is intermittent in space, i.e., it varies greatly from place to place.

The velocity increment $\Delta f(x,r) = |f(x) - f(x+r)|$ is equivalent to a wavelet transform with $\psi_\Delta(x) = \delta(x+1) - \delta(x)$. In fact Jaffard [86] has shown that the exponent $\eta(p)$ is defined by

$$\tilde{S}_p(r) = \frac{1}{L}\int_0^L |\tilde{f}(x,r)|^p dx \sim r^{\eta(p)} \qquad (30)$$

is the same as $\zeta(p)$ provided $p > 1$ and $\zeta(p) < p$, no matter what wavelet is used. The wavelet-based method of calculating the structure function unifies the analysis of structure functions with the calculation of energy spectra and the strength of local singularities. If one uses a wavelet with a sufficient number of vanishing moments, then the wavelet-based structure function $\tilde{S}_p(r)$ should also be more sensitive to larger α singularities since the equivalent wavelet for the structure function, $\psi_\Delta(x)$, has only one vanishing moment. By changing from an integral to a sum over wavelet maxima (as in Arnéodo *et al.*'s [4] wavelet maximum modulus method discussed in the following section) one can extend the definition of structure functions to include negative p's.

The wavelet-based version of the structure function allows us to see directly how the structure function is determined by the singular behavior of $f(x)$. From (13) the wavelet transform modulus is proportional to $r^{\alpha(x_0)}$ and thus, since $r < 1$, the stronger singularities contribute most to the higher order structure functions and least to the lower order structure functions. In other words, the value of $\zeta(p)$ is determined mostly by the stronger singularities for large p's and mostly by the weaker singularities for small p's.

Davis *et al.* [41] point out that the "dissipation" of a discrete function f_j, $\varepsilon_j = |f_j - f_{j-1}|$, is in fact a measure. Because ε_j is a measure, the generalized dimension $D(p)$ of $f(x)$ can be calculated from the exponent $K(p)$ of the structure function of $\varepsilon(x)$

$$D(p) = 1 - \frac{K(p)}{p-1}. \qquad (31)$$

The generalized dimension $D(p)$ is the dimension of the set containing the singularities that contribute most to the pth order structure function. Because $\varepsilon(x)$ is a stationary variable (for $1 < \beta < 3$) we have $0 < \beta_\varepsilon(x_0) < 1$ and thus $-1/2 < \alpha(x_0) < 0$. Because $\alpha(x_0) < 0$ the dissipation contains actual singular behavior (the dissipation tends to infinity).

In general terms the exponents $\zeta(p)$ characterize the stationarity of the field, while the exponents $K(p)$ characterize

Table 1 Properties of a Signal from the Behavior of the Exponents of its Structure Function $\zeta(p)$ and the Structure Function of the Modulus of its Derivative $K(p)$

Value of Structure Function	Type of Signal
$\zeta(1) = 0$	Stationary, $D_F = 2$
$\zeta(1) = 1$	Noiseless, $D_F = 1$
$K'(1) = 1$	weak variability
$K'(1) = 0$	δ–function
$\zeta(p)$ variable	nonstationary multifractal
$\zeta(p)$ constant	nonstationary monofractal
$K(p)$ variable	stationary multifractal
$K(p)$ constant	stationary monofractal

the singularity of the field. One can learn a great deal about the behavior of a signal from the variability of $\zeta(p)$ and $K(p)$ and from the value of the first structure function exponents $\zeta(1)$ and $K(1)$. This information is summarized in Table 1.

Davis *et al.* [41] introduced the "mean multifractal plane" defined as the plane with coordinates given by the most informative exponents $0 < \zeta(1) = 2 - D_F < 1$ and $0 < K'(1) = 1 - D(1) < 1$ (where D_F is the fractal dimension and $D(1)$ is the information dimension). The position of a particular flow or model on the mean multifractal plane is a good indicator of its self-similar characteristics. The higher the flow's $K'(1)$ component the more intermittent and multifractal it is, and the higher the flow's $\zeta(1)$ component, the smoother and less stationary it is. Experimental turbulent velocity fields lie in the center of the mean multifractal plane. Turbulence models, however, tend to lie along the boundaries of the domain: purely multiplicative cascade models (such as δ-functions) lie on the $K'(1)$ axis and purely additive models (such as fractional Brownian motion) lie on the $\zeta(1)$ axis! This clearly indicates that the current turbulence models do not represent correctly the self-similar structure of turbulent flows.

E. The Singularity Spectrum for Multifractals

In order to characterize a multifractal function it is necessary to calculate its *singularity spectrum*. The singularity spectrum $D(\alpha)$ may be defined as the fractal dimension of the set of points with Hölder exponent α

$$D(\alpha) = D_F\{x, \alpha(x) = \alpha\}. \tag{32}$$

Note that this definition is equally valid for multifractal functions and measures. The singularity spectrum of a monofractal has only one point, e.g., the singularity spectrum of the fractional Brownian signal $B_{1/3}(x)$ which has a $k^{-\frac{5}{3}}$ energy spectrum is $D(\alpha = 1/3) = 1$ (the function $B_{1/3}(x)$ is singular everywhere with $\alpha = 1/3$), while a the singularity spectrum of a multifractal is a curve.

Frisch and Parisi [72] found a way of estimating the singularity spectrum from the Legendre transform of the structure function exponents $\zeta(p)$

$$D(\alpha) = \inf_p(p\alpha - \zeta(p) + 1) \tag{33}$$

where, as explained in Section III-C, $\zeta(p)$ may be calculated using the wavelet transform.

Equation (33) can be derived heuristically by noticing that near a singularity of order α

$$|\tilde{f}(x, r)| \sim r^{\alpha p} \tag{34}$$

where we have used (13) and have written $\alpha = \alpha(x_0)$ for simplicity. Now, if the dimension of the points with singularity α is $D(\alpha)$ then there are about $r^{-D(\alpha)}$ "boxes" (in this case wavelets) with the scaling (34) in each interval r, so that the total contribution to the integral (30) is $r^{\alpha p - D(\alpha)+1}$. To leading order the magnitude of the integral is given by the largest contribution so that

$$\zeta(p) = \inf_p(\alpha p - D(\alpha) + 1). \tag{35}$$

Since $\zeta(p)$ is concave, formula (33) can be obtained by an inverse Legendre transform.

Jaffard [86] proved mathematically, however, that structure function calculations of the singularity spectrum can, in general, only set a upper bound on $D(\alpha)$ and he gave some counterexamples where such calculations give completely misleading answers.

Arnéodo *et al.* [4] have developed a method for calculating the singularity spectrum called the wavelet transform modulus maximum (WTMM) method. This method is closely related to the calculation of structure functions by wavelet transforms except that, instead of integrating (or summing in case of discretely defined functions) the wavelet transform over all positions, one only sums the wavelet transforms located at maxima, i.e.,

$$\tilde{\Sigma}_p(r) = \sum_{l \in L(r)} \left(\sup_{(x,r')} |\tilde{f}(x, r')|^p \right) \tag{36}$$

where l is a maxima line of the wavelet transform modulus on $[r, 0]$ and $\sup_{(x,r')}$ means that the supremum is taken for (x, r') on l (so that $r' \leq r$). The wavelets are in fact playing the role of "generalized boxes" in a new form of the standard box-counting algorithm used to estimate fractal dimensions $D(\alpha)$. Summing only over the wavelet modulus maxima makes sense since, as Mallat and Hwang [114] showed, most of the information in the wavelet transform is carried by the wavelet maxima lines. Furthermore, because one does not sum over places where the wavelet modulus is zero $\tilde{\Sigma}_p(r)$ is also defined for $p < 0$ as well as for $p \geq 0$. Note that the structure function methods are defined only for $p \geq 0$.

Arnéodo *et al.* draw the analogy with statistical thermodynamics and interpret $\tilde{\Sigma}_p(r)$ as a "partition function" (see Table 2).

Table 2 Analogies between Statistical Thermodynamics and the Wavelet Transform Modulus Maximum method for Multifractals

Thermodynamic parameter	Multifractal parameter
T (temperature)	p^{-1}
Z (partition function)	$\tilde{\Sigma}_p(r)$
G (free energy)	$\tau(p)$
S (entropy)	$D(\alpha)$

If $f(x)$ is a self-similar function then $\tilde{\Sigma}_p(r) \propto r^{\tau(p)}$ and the singularity spectrum can be found by calculating the Legendre transform

$$D(\alpha) = \inf_p(p\alpha - \tau(p)). \tag{37}$$

To avoid technical problems associated with calculating the Legendre transform in (37) Arnéodo *et al.* [4] recommend an alternative way of finding $D(\alpha)$.

Jaffard [86] proved mathematically that the WTMM method, unlike the structure function methods, gives the correct singularity spectrum for all p provided it is slightly

modified. Indeed a problem might arise if the wavelet modulus maxima are too close together; in that case the sum in an interval of width r must be restricted to the largest maxima. Jaffard also shows that even the modified WTMM method fails if the function $f(x)$ contains too many oscillating singularities.

Arnéodo *et al.* [4] find the relation between $\tau(p)$ and $\zeta(p)$ from their respective definitions in terms of $D(\alpha)$, but given the limitations of (33) it is perhaps better (and more intuitive) to find the connection directly through the structure functions. In terms of discrete signals, the wavelet transform-based calculation of the structure function (30) becomes

$$\tilde{S}_p(r) = \frac{1}{N} \sum_{j=1,N} |\tilde{f}(x_j, r)|^p. \tag{38}$$

Each cone of influence of width r must contain only maxima lines with the same scaling (since the scaling $r^{\alpha(x_0)}$ is the same for all points within the influence cone of point x_0) and if the function is everywhere singular all intervals of size r must contain at least one maxima line. If one follows Jaffard's [86] refinement to WTMM, and only counts one maximum for each interval of length r, then the number of terms in the sum must be proportional to N/r. Therefore, if the wavelet moduli are only summed over their maxima the structure function becomes

$$\tilde{S}_p(r) = \frac{1}{N/r} \sum_{l \in L(r)} \left(\sup_{(x_j, r')} |\tilde{f}(x_j, r')|^p \right) = \frac{1}{N/r} \tilde{\Sigma}_p(r). \tag{39}$$

We thus find that the relation between the structure function exponents $\zeta(p)$ and the WTMM "free energy" exponents $\tau(p)$ is

$$\zeta(p) = \tau(p) + 1. \tag{40}$$

Note that (40) only holds if the function $f(x)$ has singularities everywhere and WTMM is modified by only counting one wavelet modulus maximum for each interval of length r.

Arnéodo *et al.* [4] applied the WTMM method to single point high Reynolds number (the Taylor scale based Reynolds number is $R_\lambda = 2720$) velocity data obtained by Gagne [78] from the wind tunnel of ONERA at Modane. The self-similar inertial range follows the Kolmogorov $E(k) \sim k^{-\frac{5}{3}}$ law for almost three decades. The WTMM analysis was carried out for this inertial range of scales on a section of data 100 integral (energy containing) scales long.

The histogram of singularities $\alpha(x_0)$ in the turbulence data was found to be quite wide and centered about the Kolmogorov value $\alpha = 1/3$. Surprisingly, at some places in the flow α is negative which implies actual singular behavior (velocity tending toward infinity). These negative α values may be spurious or may indicate the (rare) presence of strong vortices. The function $\tau(p)$ is convex which suggests that the regularity of the flow varies greatly from place to place. The singularity spectrum is peaked at the Kolmogorov value $\alpha_{\max}(p = 0) = 0.335 \pm 0.005$ with $D(\alpha_{\max}) = 1.000 \pm 0.001$. This result indicates that the signal is fractal everywhere because the fractal support of $D(\alpha_{\max})$ is equal to its topological dimension (i.e., the dimension of the signal, which is one).

Arnéodo *et al.* [4] come to the conclusion that turbulence is singular with a multifractal spectrum of singularities centered around the Kolmogorov value $\alpha = 1/3$ and is therefore not homogeneous.

F. Distinguishing Between Signals Made up of Isolated and Dense Singularities

Although the inertial range of turbulence has a self-similar structure, not all self-similar functions are fractal; in fact one of the most physically plausible turbulence structures, the spiral vortex, can generate self-similar oscillating singularities with a nontrivial box-counting dimension. The conclusion drawn by Arnéodo *et al.* [4] that turbulence is everywhere singular with a multifractal structure may be invalid if the turbulent velocity signal they analyzed contains oscillating singularities. Because the WTMM method is only valid for signals that contain dense distributions of cusp type singularities, one should first try to determine whether a signal has isolated oscillating singularities before attempting to use the WTMM method. Unfortunately, the difference between signals containing singularities everywhere ("fractals") and signals containing a large number of isolated oscillating singularities (isolated "spirals" in multidimensions or isolated "chirps" in 1-D) is not obvious: both signals can have nontrivial box-counting dimensions.

Kevlahan and Vassilicos [91] developed two methods for distinguishing between isolated spiral and fractal signals based on the wavelet transform. (In fact their method only distinguishes between isolated and dense singularities, however, isolated cusp singularities have a trivial box-counting dimension and thus can be distinguished from fractal signals on the basis of box-counting dimension alone.) The first method takes advantage of the fact that the singularities in a fractal are dense (there are singularities at all points) whereas the singularities in an isolated spiral signal are isolated (the signal contains oscillating singularities only at the centers of spirals). If one averages the wavelet transforms of many realizations, or different data segments together, one can prove that the average wavelet transform modulus $\langle |\tilde{f}(x,r)| \rangle$ decays differently for the two types of singularity as

$$\langle |\tilde{f}(x,r)| \rangle \propto N^{-1/2} |\tilde{f}(x_0, r)| \tag{41}$$

for fractal signals but as

$$\langle |\tilde{f}(x,r)| \rangle \propto |\tilde{f}(x_0, r)| r < L/N \tag{42}$$

for spiral signals where N is the number of segments averaged together and L is the length of each segment. Thus the average wavelet transform of the random phase fractal signal is $N^{-1/2}$ times a single realization, while that of the spiral signal does not depend on the number of realizations below a certain scale. The difference in the behavior of $\langle |\tilde{f}(x,r)| \rangle$ is striking, and provides a

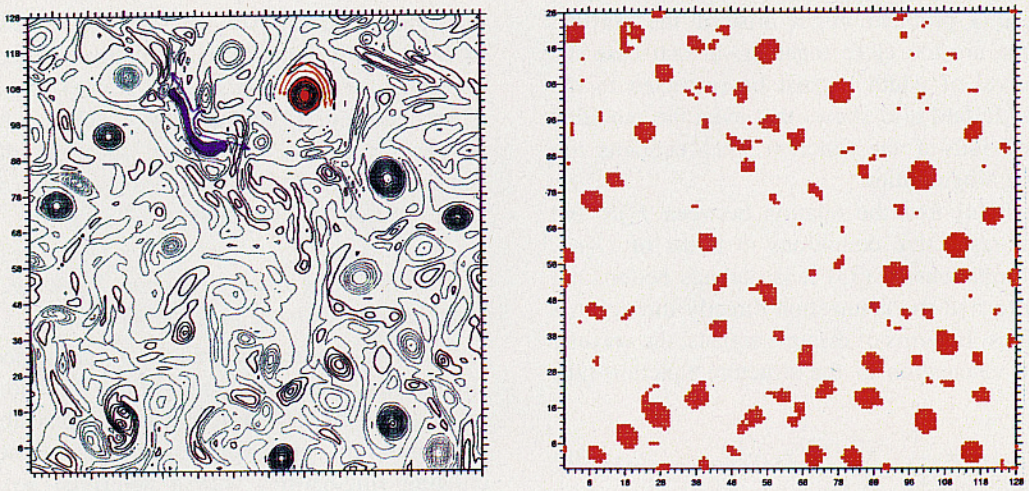

(a) (b)

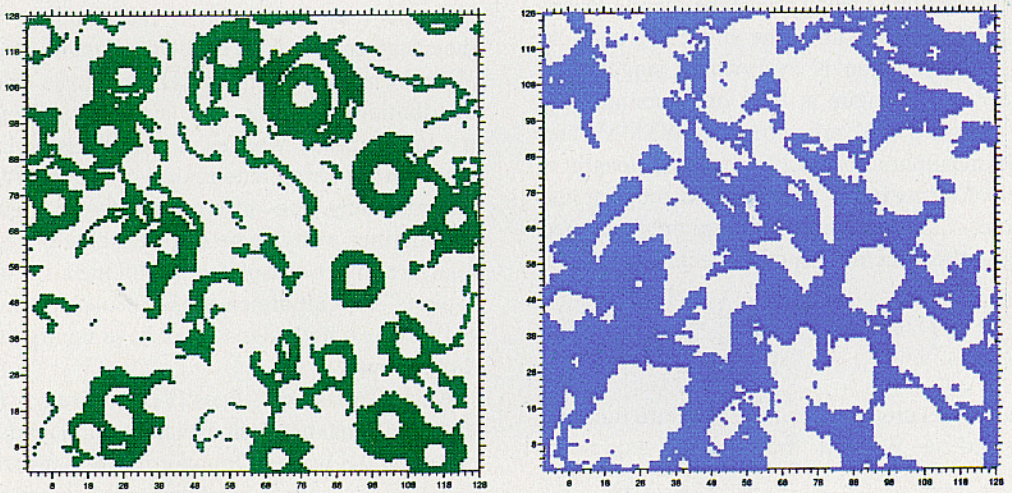

(c) (d)

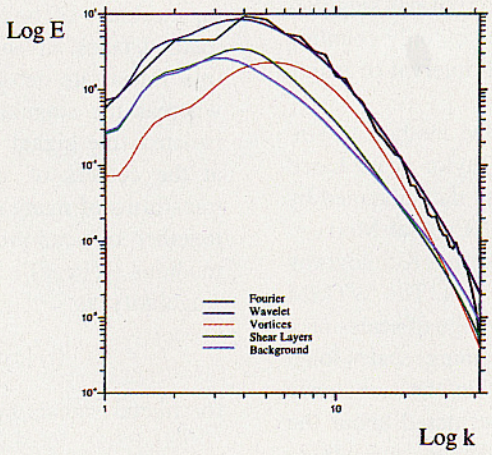

(e)

Fig. 2. Conditional wavelet spectra (this computation was done in collaboration with T. Philipovitch). (a) Vorticity field. In red: elliptic regions, dominated by rotation, wich correspond to the coherent vortices. In blue: hyperbolic regions, dominated by deformation, which correspond to the incoherent background flow. (b) Coherent vortices, (c) shear layers, (d) background flow, and (e) energy spectra. In black: Fourier energy spectrum, which scales as k^{-5}. In dark blue: wavelet energy spectrum, which is a smooth approximation of the Fourier spectrum and scales as k^{-5}. In red: wavelet energy spectrum of the coherent vortices, which scales as k^{-6}. In green: wavelet energy spectrum of the shear layers, which scales as k^{-4}. In light blue: wavelet energy spectrum of the background flow, which scales as k^{-3}.

diagnostic for determining whether a signal contains spiral-type singularities. This method was applied to the Gagne [78] turbulence data. The results were inconclusive, perhaps due to insufficient resolution near expected spiral scales or rarity of spiral vortices passing near the velocity probe.

The second method for distinguishing between isolated spiral and fractal singularities derives from the observation that the spatial fluctuation of wavelet energy $\tilde{E}(x,k)$ (measured by the standard deviation $\tilde{\sigma}(k)$ of $\tilde{E}(x,k)$) is independent of wavenumber for a random phase fractal signal, but increases with wavenumber for a spiral signal with the same energy spectrum. Analysis of the turbulent signal shows that $\tilde{\sigma}(k)$ increases with wavenumber (although at a slower rate than for the purely spiral test signal), indicating that turbulence probably contains some sort of isolated oscillating singularities. This conclusion should be borne in mind when interpreting the results of multifractal analyses of turbulence.

IV. Turbulence Analysis

A. New Diagnostics Using Wavelets

It is impossible to define a local Fourier spectrum, because Fourier modes are nonlocal, but it is possible to define a *local wavelet spectrum*, since wavelets are localized functions. Actually, due to the inherent limitation of the uncertainty principle stating that there is a duality between spectral and spatial information, we should be aware that the spectral accuracy will be poor in the small scales and that the spatial accuracy will be poor in the large scales.

Since turbulent flows are either 2-D or 3-D, in the following section we will use the 2-D wavelet transform. Let us consider a 2-D scalar field $f(\mathbf{x})$ and a 2-D real isotropic wavelet $\psi(\mathbf{x})$. We generate the family $\psi_{\mathbf{x},r}(\mathbf{x}')$ of wavelets, translated by position parameter $\mathbf{x} \in R^2$, and dilated by scale parameter $r \in R^+$, all having the same L^2 norm

$$\psi_{\mathbf{x},r}(\mathbf{x}) = r^{-1}\psi\left(\frac{\mathbf{x}'-\mathbf{x}}{r}\right). \tag{43}$$

The 2-D wavelet transform of $f(\mathbf{x})$ is

$$\tilde{f}(\mathbf{x},r) = \int_{R^2} f(\mathbf{x}')\,\psi_{\mathbf{x},r}(\mathbf{x}')\,d^2\mathbf{x}'. \tag{44}$$

The local wavelet spectrum of $f(\mathbf{x})$ is defined as

$$\tilde{E}(\mathbf{x},r) = \frac{|\tilde{f}(\mathbf{x},r)|^2}{r}. \tag{45}$$

A characterization of the local "activity" of $f(\mathbf{x})$ is given by its *wavelet intermittency* $\tilde{I}(\mathbf{x},r)$, which measures local deviations from the mean spectrum of f at every position $\mathbf{x}$ and scale r, defined as follows

$$\tilde{I}(\mathbf{x},r) = \frac{|\tilde{f}(\mathbf{x},r)|^2}{\int_{R^2}|\tilde{f}(\mathbf{x},r)|^2\,d^2\mathbf{x}}. \tag{46}$$

Another measure of interest for turbulence is the *wavelet Reynolds number* $\tilde{\mathrm{Re}}(\mathbf{x},r)$, given by

$$\tilde{\mathrm{Re}}(\mathbf{x},r) = \tilde{u}(\mathbf{x},r)\frac{r}{\nu} \tag{47}$$

where r is the scale parameter, ν the kinetic viscosity of the fluid, and $\tilde{u}$ the root-mean-square (rms) value of the velocity field contribution at position $\mathbf{x}$ and scale r defined as

$$\tilde{u}(\mathbf{x},r) = \left(\frac{1}{3C_\psi}\sum_{i=1}^{3}|\tilde{\mathbf{u}}_i(\mathbf{x},r)|^2\right)^{1/2}. \tag{48}$$

with the constant

$$C_\psi = \int_{R^2}|\hat{\psi}(\mathbf{k})|^2\frac{d^2\mathbf{k}}{|\mathbf{k}|^2}. \tag{49}$$

The expectation is that at large scales $r \sim L$, the wavelet Reynolds number should coincide with the usual large-scale Reynolds number $\mathrm{Re} = uL/\nu$, where u is the rms turbulent velocity and L is some integral scale of the flow. In the smallest scales (say $r \sim \eta$, where η is the Kolmogorov scale of the flow), one expects this wavelet Reynolds number to be close to unity when averaged spatially. The question we want to address here is the variability of such a wavelet Reynolds number defined for space and scale: are there locations where such a Reynolds number at some small scale is much larger than in others, and how do such regions correlate with regions of small-scale activity in the flow? If so, then $\tilde{\mathrm{Re}}(\mathbf{x},r)$ gives an unambiguous measure of the activity at small scales (or at any desired scale). Such regions of high wavelet Reynolds number could then be interpreted as regions of strong nonlinearity.

Concerning the computation of energy and enstrophy transfers and fluxes, we should be aware that the results depend on the functional basis we consider. Indeed, due to Heisenberg's uncertainty principle, each representation measures different types of transfers and fluxes. In Fourier space one computes transfers between different independent wavenumber bands, which detect the modulations and resonances excited under the flow dynamics. In wavelet space one computes exchanges between different locations and different scales, which detect instead advections and scalings. But one should never forget that in wavelet space spatial resolution is bad in the large scales while scale resolution is bad in the small scales. In an orthogonal wavelet basis, although all wavelets are independent in space and scale, they are not independent in wavenumber. In an orthogonal wavelet packet basis all wavelet packets are independent in space, scale, and wavenumber, but their spectrum presents several peaks at distant wavenumbers and they are no longer local in wavenumber space; therefore wavelet packets are unable to precisely measure transfers between different wavenumber bands. This is the reason why a comparison between transfers computed in wavelets, in wavelet packets, and in Fourier modes is misleading: these three diagnostics do not measure the same quantities!

B. Two-Dimensional Turbulence Analysis

Unlike the velocity field, the vorticity field is invariant with respect to uniform rectilinear translations of the inertial frame (Galilean invariance). The dependence of streamlines

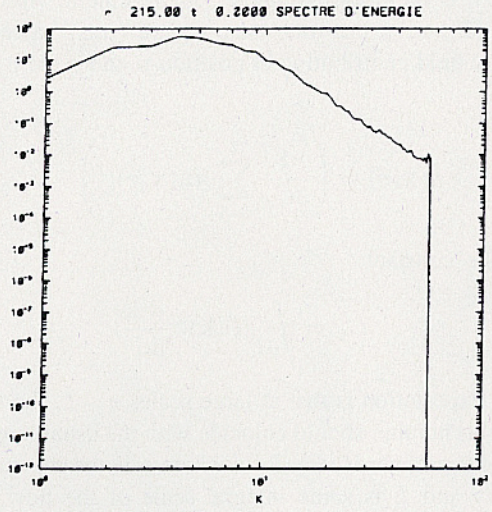

(a)

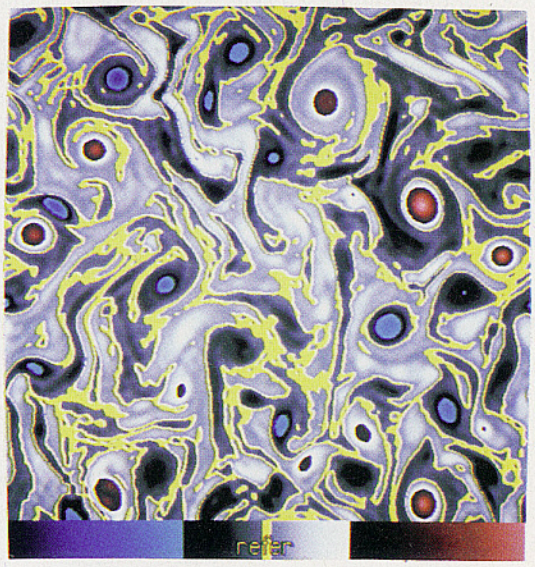

(b)

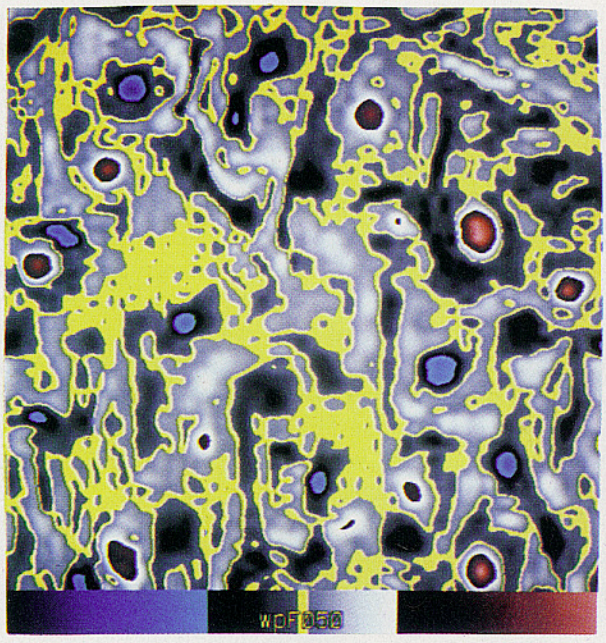

(c)

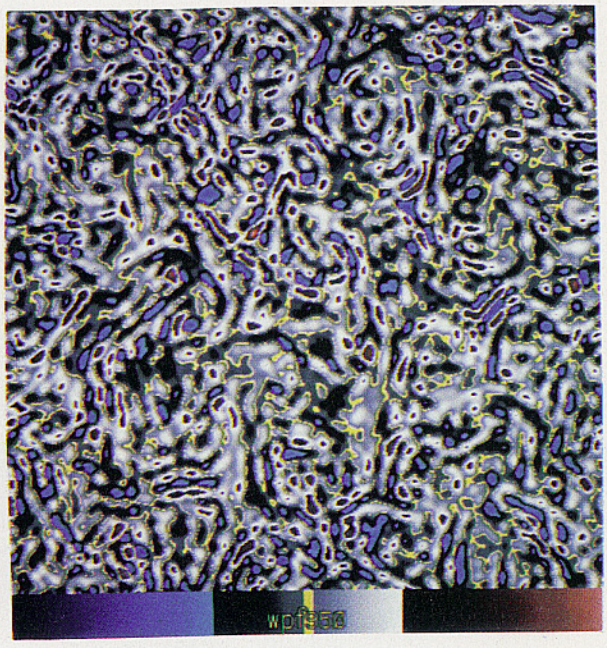

(d)

Fig. 3. (a) The uncompressed vorticity field and its Fourier spectrum which scales as k^{-5}. (b) The vorticity field reconstructed from the 5% strongest wavelet packet coefficients, which contains 89% of the total enstrophy, and its Fourier energy spectrum which scales as k^{-6}. (c)(d) The vorticity field reconstructed from rest of the flow (95% of wavelet packet coefficients) which contain 11% of the total enstrophy, and its Fourier energy spectrum which scales as k^{-3}.

and streaklines on the reference frame causes considerable difficulties in the study of fluid flows, particularly in observing and defining vortices. In fact due to its Galilean invariance, vorticity is the most suitable field for tracking the dynamics of turbulent flows, in both two and three dimensions. The vorticity field is directly accessible from numerical simulations, but is difficult to obtain from laboratory experiments. This is why we will now focus on vorticity fields obtained from DNS results. The drawback with DNS, i.e., the integration of Navier–Stokes equations without any *ad hoc* turbulence modeling, is that current supercomputers are only able to compute low Reynolds number flows (up to a few thousand).

Let us show an example of a wavelet analysis of an instantaneous vorticity field computed using the Navier–Stokes equations [134], [60]. We segment it into three regions using the Weiss criterion [158], [52], namely into *rotational regions* corresponding to the coherent structures, *strongly strained regions* corresponding to the shear layers surrounding the coherent structures, and

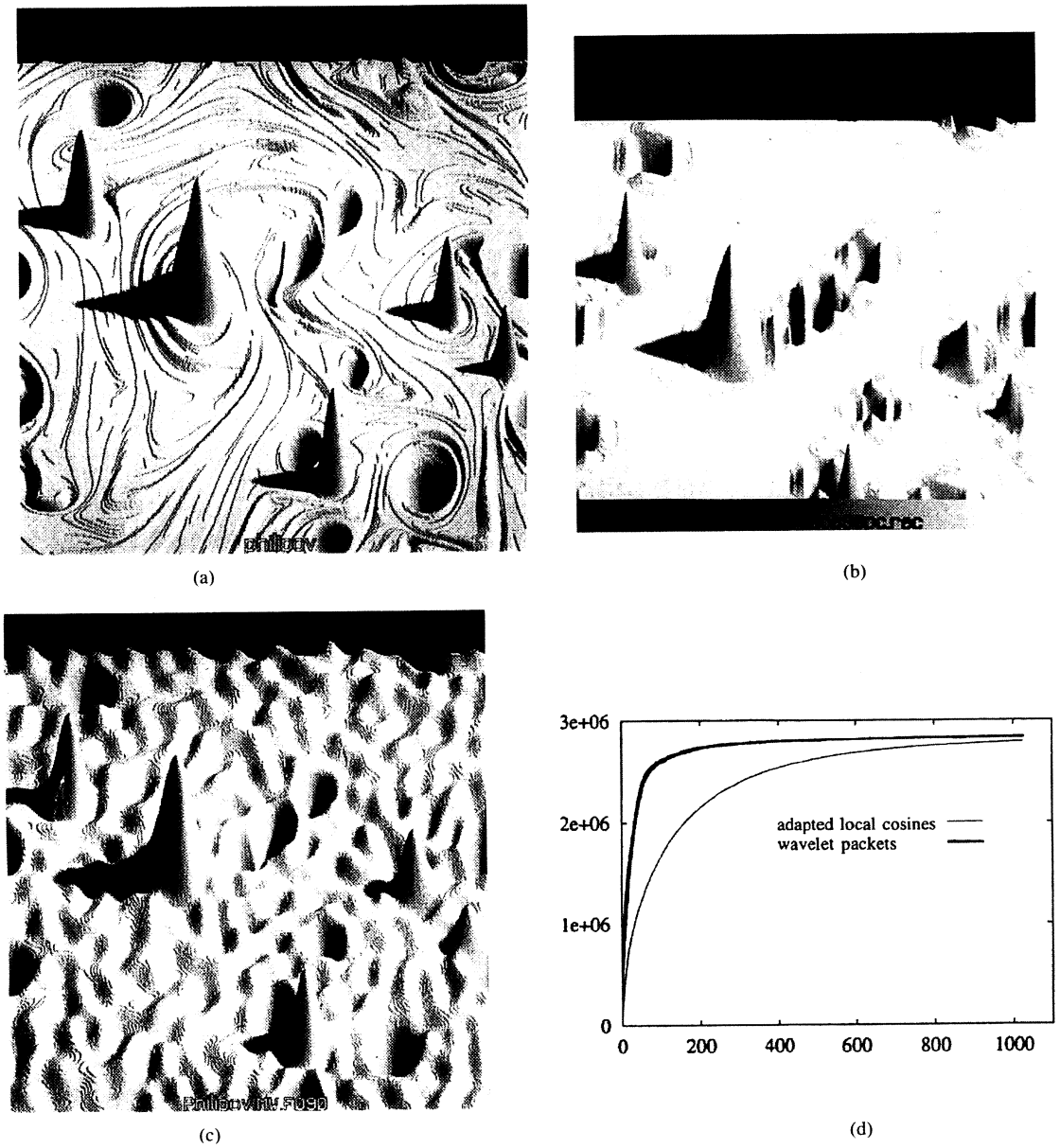

Fig. 4. Comparison between wavelet packet and adapted local cosine compression (this computation was done in collaboration with Echeyde Cubillo). (a) The uncompressed vorticity field. (b) The vorticity field reconstructed from the 70 strongest wavelet packet coefficients, which contain 90% of the enstrophy. (c) The vorticity field reconstructed from the 425 strongest adapted local cosine coefficients, which contain 90% of the total enstrophy. (d) Enstrophy contained in the retained coefficients versus their number. We observe, for instance, that 70 wavelet packet coefficients retain 90% of the total enstrophy, while 70 adapted local cosine coefficients retain only 50% of the total enstrophy.

weakly strained regions corresponding to the background flow made of vorticity filaments (these vorticity filaments encountered in 2-D turbulence are not the same dynamical objects as the vorticity tubes encountered in 3-D turbulence and often called filaments). We then decompose the vorticity field into a continuous wavelet representation using an isotropic (Hermite) wavelet to integrate in space the wavelet coefficients for each type of region. This decomposition is in fact a conditional statistical analysis because the energy spectrum is computed separately for each type of region.

The energy spectrum of the *coherent structure regions* tends to scale as k^{-6}, the *sheared regions* as k^{-4} and the *background regions* as k^{-3} (Fig. 2). We found that each region has energy throughout the inertial range and therefore there is no scale separation [134], [60]. This is why the Fourier representation cannot disentangle these different regions. The scaling of the coherent structures seems compatible with the cusp-like model proposed by Farge and Holschneider [64], the scaling of the shear layers seems compatible with the k^{-4} spectrum predicted by Saffman [147] and only the scaling of the homogeneous background

regions seems to verify the Batchelor–Kraichnan prediction of a k^{-3} spectrum. From this analysis we confirm that there is no universal power-law scaling for 2-D turbulent flows; the slope of the Fourier energy spectrum varies with the density of coherent structures (their number per unit area in 2-D and per unit volume in 3-D), which depends on initial conditions and forcing (energy injection by external forces). We then conjecture that there may be a universal scaling for each region of the flow considered separately, but this has not yet been proven. Extensive wavelet analysis of very different types of turbulent flows would be necessary to check this conjecture.

The new approach we propose is to decompose turbulent flows into organized (and therefore inhomogeneous) components and random (and therefore homogeneous) components, which will have different scalings and different statistical properties; namely the former would be Gaussian while the latter would be non-Gaussian. If this point of view is confirmed, then only conditional averaging will make sense. There is still some hope of finding an universal behavior for each component taken separately, and we may then be able to design a new statistical theory of 2-D turbulence based on this property.

A key question, which remains open, is the following: is there a generic shape (namely a typical vorticity distribution) for coherent structures? The answer to this question influences our analysis, in particular our interpretation in terms of scale, because the notion of scale is intrinsically linked to the generic shape we assume for the coherent structures. *A prioris* are as essential in statistical analysis as hypotheses are in modeling: we should state them clearly, otherwise our results will be nonsensical. For instance, without a definition of vortex shape the notion of vortex size and vortex circulation would be meaningless. A misunderstanding has persisted for years in the field of turbulence due to the identification of scale with the inverse wavenumber, which is true only if one assumes a wavelike shape for the vorticity field. Conversely, in other papers one encounters different implicit models of coherent structures (vortex patches, Gaussian vortices, or cusplike vortices), which indeed condition our statistical analysis. Therefore one first needs a method to extract coherent structures out of turbulent flows in order to study them individually. The classical method consists of thresholding the vorticity field and identify as coherent vortices all regions where vorticity is larger than this threshold. However, the spectral information is then lost due to the discontinuity introduced by the threshold. We have proposed instead [66] two new methods based on the continuous wavelet representation, which preserves the regularity of the vorticity field and therefore its spectrum.

These methods depend on the choice of the analyzing wavelet and ideally we should use a wavelet which is a local solution of the linearized Navier–Stokes equations, namely a solution of the heat equation, such as any isotropic and smooth distribution of vorticity. This is why we use 2-D Hermite wavelets (derivatives of the Gaussian), which are solutions of the heat equation. The higher the derivative, the better the cancellations and the more sensitive the wavelet will be to quasi-singular vortices, however its spatial selectivity will not be as good as for low order derivative wavelets. In the example shown in this paper we use Marr's wavelet which is the Laplacian of the Gaussian.

The first method is to retain only the wavelet coefficients inside the influence cones (namely the spatial support of the wavelets) attached to the local maxima of the vorticity field corresponding to the centers of coherent structures; wavelet coefficients outside the influence cones are then discarded before reconstructing the vorticity field. The second method is to retain only the wavelet coefficients which are larger than a given threshold and to discard all other coefficients before reconstructing the vorticity field. We thus extract the coherent structures, and substracting the original vorticity field gives us the background field. By computing the Fourier spectrum of these two fields we have confirmed our previous analysis: the energy spectrum of coherent structures tends to scale as k^{-6} and that of the background field as k^{-3} (Fig. 3). With our first method we can also extract just one coherent structure, analyze its shape, and compute its coherence function, namely the pointwise relation between vorticity and streamfunction, to check if it corresponds to the stationary states predicted by Montgomery's [90] or by Robert's [143]–[145] statistical theories. We are presently working in this direction, but have not yet published any result.

Another application of the wavelet representation in turbulence should be to design new types of forcing for numerical simulations. The method would consist of inject energy and enstrophy at each time step, but only into the wavelet coefficients inside the influence cone corresponding to a given location. Depending on the type of forcing we want, we could either excite the same vortices or randomly select new vortices at each time step. Forcing is currently done in Fourier space and is rather unphysical, while wavelet-based forcing could simulate the production of vorticity in boundary layers or mixing layers, which is a local process. This is another promising, but as yet untried, application of wavelet techniques for turbulent flow simulation.

C. Three-Dimensional Turbulence Analysis

We have analyzed different flow fields resulting from DNS of 3-D turbulent flows [63], using the complex-valued Morlet wavelet, which plays the role of a numerical polarizor due to its angular selectivity, and whose complex modulus directly measures the energy density. We have first studied the temperature, velocity, and pressure fields of a channel flow near the wall and have used the wavelet intermittency to pinpoint the regions of the flow dominated by strong nonlinear dynamics. It appears that the most intermittent regions are correlated with those of large vertical velocity, corresponding to ejections from the boundary layer. We have found that temperature behaves as a passive scalar almost everywhere, except in these very localized regions. We have also observed that there is no

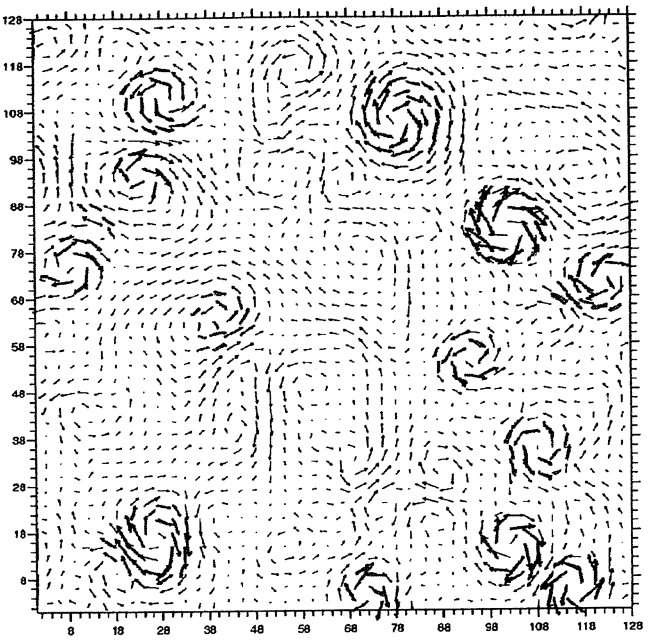

(a)

Fig. 5. Wavelet Reynolds number (this computation was done in collaboration with T. Philipovitch). (a) Velocity field computed with resolution 128^2 ($\Delta x = 1$ unit length between two grid points).

return to isotropy in the small scales, contradicting one of the hypotheses of the statistical theory of turbulence, which supposes that turbulent flows become homogeneous and isotropic at small scales.

We have then analyzed the vorticity, velocity and a passive scalar in a temporal mixing layer after the mixing transition. We have found that wavelet intermittency is very strong—up to 120—in the collapsing regions where the ribs (streamwise vorticity tubes produced by a 3-D instability) are stretched and engulfed into the primary spanwise vortex (produced by a 2-D Kelvin–Helmholtz instability). On the other hand, the wavelet intermittency in the braids, i.e., outside the spanwise vortex, remains very low, not exceeding five. We have also noticed a return to isotropy in the small scales. From the local spectrum of the vertical vorticity we have observed that the collapsing regions have a spectral slope much shallower than one of the braid regions; this departure from the space average wavelet spectrum increases with the scale and confirms the strong intermittency of the mixing layer. If we extrapolate the observed slopes, we conjecture that intermittency should increase with Reynolds number. We have then visualized the iso-surfaces of the wavelet Reynolds number, which can be interpreted as surfaces of iso-nonlinearity in the flow. The peaks on these iso-surfaces, which are associated with the most unstable regions, are located in the primary vortex core; this confirms our previous conclusions concerning the concentration of small-scale nonlinear activity there due to the stretching of the ribs rolled around the primary vortex. We have also shown that the Kolmogorov scale, corresponding to the iso-surface $\mathrm{Re}(\vec{x}, r) \simeq 1$ where linear dissipation balances nonlinear advection, varies with location, being at much smaller scale in the vortex core than in the braids, with a scale variation of four octaves. This means that there should be some (spatially localized) dissipation for scales belonging to the inertial range. This observation contradicts Kolmogorov's hypothesis of nondissipative energy transfers in the inertial range; but is in agreement with Castaing's theory of turbulence [32], [33], with Frisch and Vergassola's [76] multifractal model and with Benzi *et al.*'s [19] extended self-similar model, which assume a weak dissipation in the inertial range.

For shear flows, such as the channel flow or the mixing layer we have studied, there is a clear correlation between large-scale events and small-scale activity, due to the presence of coherent structures. Wavelet analysis has been an essential tool for identifying them as phase-space regions correlated in both space and scale, where intermittency increases with scale [63]. We conjecture that for large Reynolds numbers these regions may become more and more localized and very intense in small-scale enstrophy. Therefore they are susceptible to develop singularities at very large Reynolds numbers. For the mixing layer these quasi-singular regions correspond to collapsing events, where the ribs are stretched and accumulated inside the primary vortex core, while for the channel flow these regions correspond to the tip of the horseshoe vortices ejected from the wall boundary layer. According to the Cafarelli–Kohn–Nirenberg theorem [29], singularities, if they exist, should be at most a set of Hausdorf measure zero for any (in particular arbitrarily large) Reynolds numbers. Therefore if we want to look for quasi-singularities in

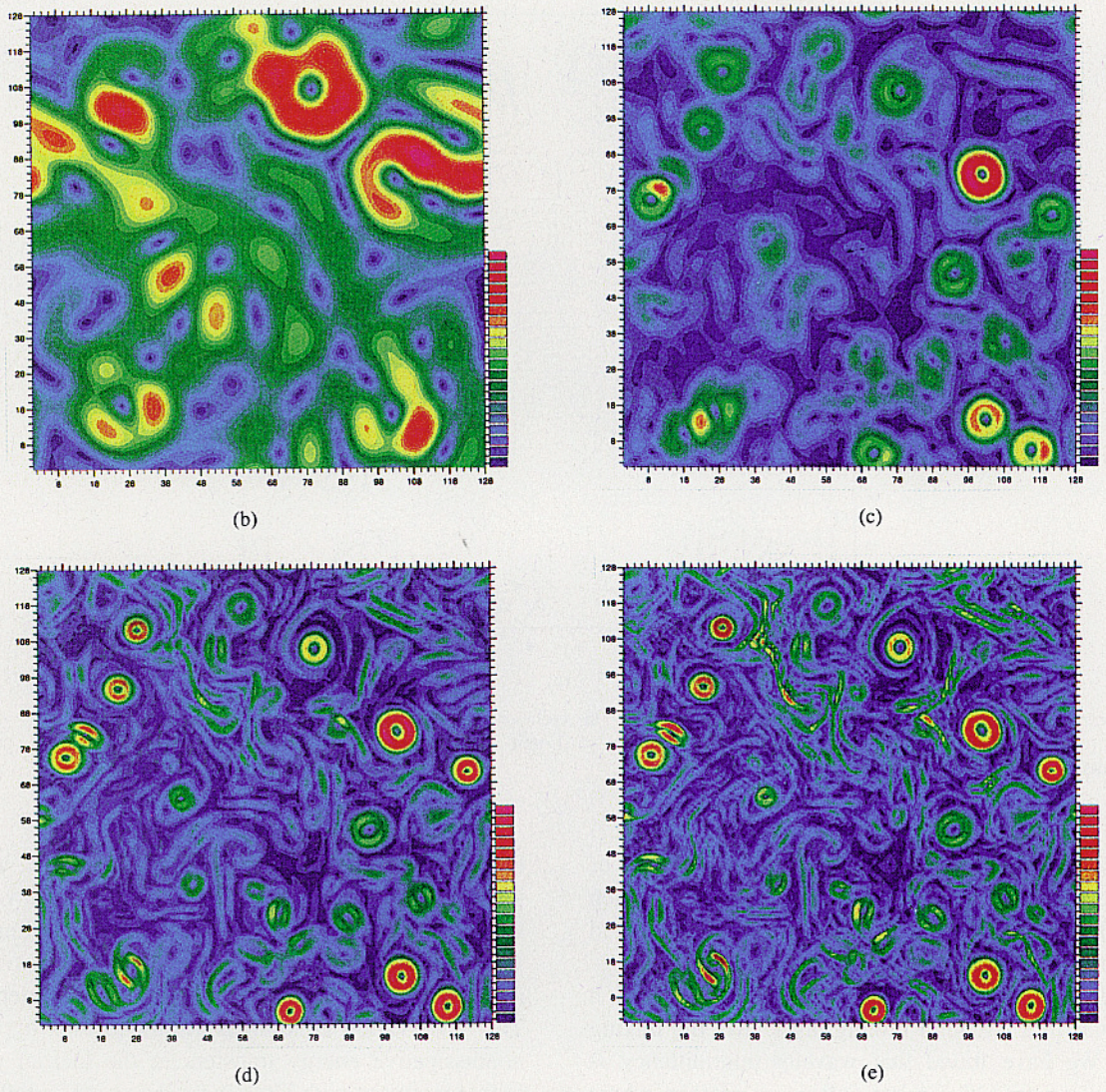

Fig. 5. (Continued). (b) Wavelet Reynolds number at scale $64\Delta x$, which fluctuates between 148 and 2700 with a mean value of 1713. (c) Wavelet Reynolds number at scale $20\Delta x$, which fluctuates between 31 and 578 with a mean value of 365. (d) Wavelet Reynolds number at scale $8\Delta x$, which fluctuates between one and 27 with a mean value of 17. (e) Wavelet Reynolds number at scale $2\Delta x$, which fluctuates between zero and three with a mean value of two.

3-D turbulent flows it would be better to use a space-time continuous wavelet transform, whose theory is being developed by Duval–Destin and Murenzi [50].

V. Turbulence Modeling

We will now reconsider the closure problem mentioned in Section II-C, taking advantage of the new observations we have made of turbulent flows, and in particular the dynamical role of coherent structures, using the wavelet analysis.

A. Two-Dimensional Turbulence Modeling

To compute turbulent flows we must separate the active components, responsible for their chaotic behavior (namely sensitivity to initial conditions), from the passive components, which are advected by the velocity field resulting from the overall coherent structure motion. The active components are not in thermal equilibrium, while the passive components are well thermalized. Therefore the active components should be computed explicitly, while the passive components can be modeled by some *ad hoc* parametrization.

Classical numerical techniques (Galerkin methods [82], large eddy simulation [107], [109], [140], and nonlinear Galerkin methods [117]) assume that the active components are the low-wavenumber Fourier modes, or the scales resolved by the computational grid, while the passive components are the high-wavenumber Fourier modes, or the subgrid scales. This scale separability of the turbulent dynamics is assumed to be true in both 2-D and 3-D.

We have shown [159] that a compression in the wavelet packet representation extracts the coherent structures out of the background flow, while the same amount of compression done in the adapted local cosine (Malvar) representation, which is a type of windowed Fourier basis, does

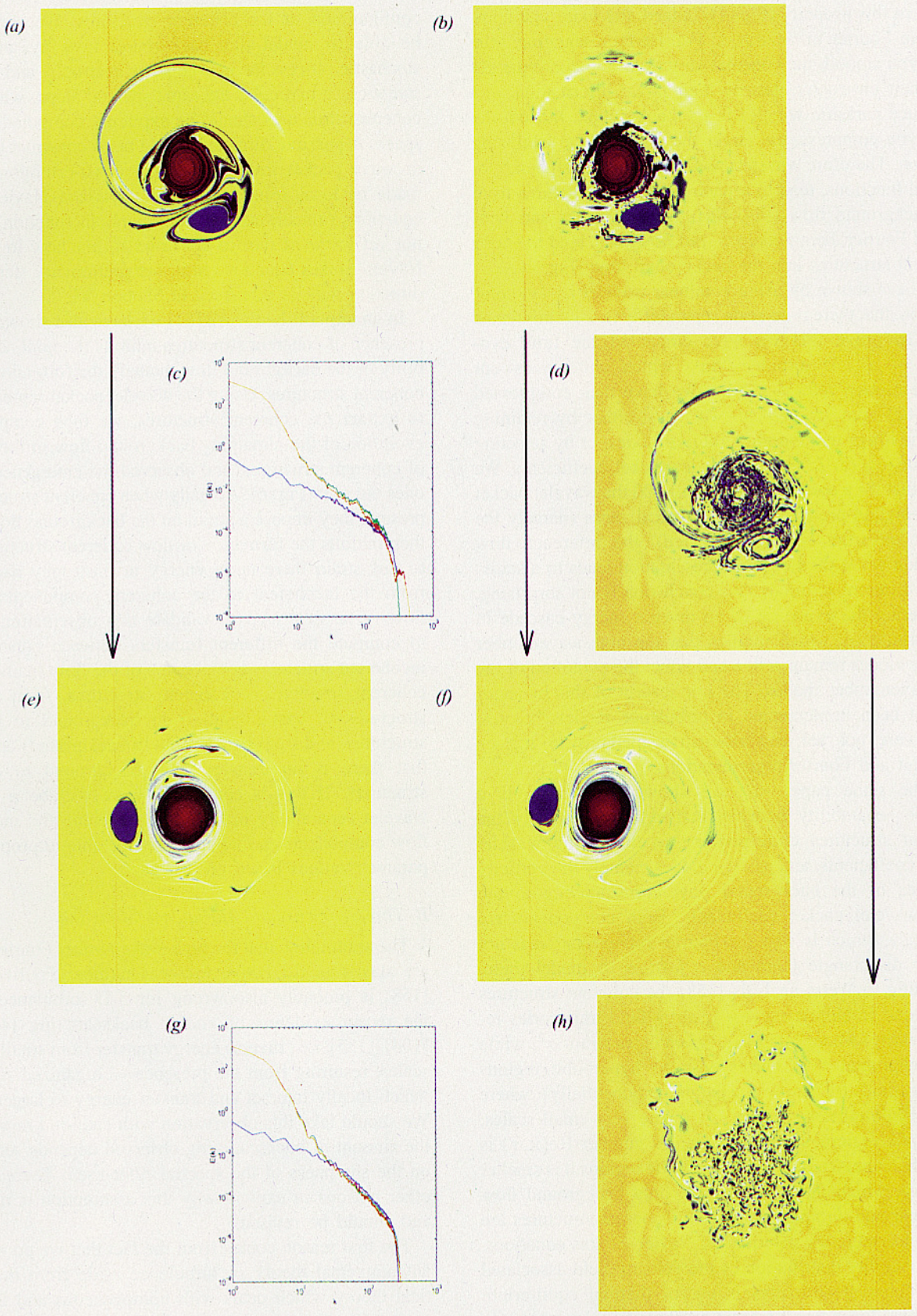

Fig. 6. Dynamical analysis of coherent structures and incoherent background flow. Green is the total energy spectrum, red is the coherent vortices energy spectrum, and blue is the filament energy spectrum. (a) Total vorticity at $t = 30$ computed with a resolution 1024^2. (b) Vorticity corresponding to the coherent vortices alone at $t = 30$. They consist of 928 strong wavelet packet coefficients which contain 95% of the total enstrophy. (c) Energy spectra at $t = 30$. (d) Vorticity corresponding to the filaments alone at $t = 30$. They consist of 932 573 weak wavelet packet coefficients which contain 5% of the total enstrophy. (e) Integration of the total vorticity until $t = 120$. (f) Integration of the coherent vortices alone until $t = 120$. (g) Energy spectra at $t = 120$. (h) Integration of the filaments alone until $t = 120$.

not have this property (Fig. 4). Indeed, the more you compress in Fourier or windowed Fourier representations, the more you smooth the coherent structures and consequently lose their enstrophy, destroy their phase information, and introduce parasitic wiggles in the background. Indeed, the more you compress, the larger the effect of the analyzing function. Therefore wavelets and wavelet packets, being localized functions, tend to separate coherent structures from the background flow (Fig. 4(b)), while Fourier and windowed Fourier, being nonlocalized functions, tend to smear coherent structures into the background flow (Fig. 4(c)).

We have shown by using nonlinear wavelet packet compression, that there is no scale separability in 2-D turbulence [62]. To prove this we have computed the time evolution of a 2-D turbulent flow which we use as our high-resolution reference flow. We have then compressed the initial vorticity field in two ways: either by retaining only the lower wavenumber Fourier modes, or by selecting the strongest (in L^2-norm) wavelet packet coefficients. We found that for a compression ratio of 200 the wavelet packet representation preserves, in a statistical sense (namely the energy spectrum is well predicted), the reference flow evolution while the Fourier representation leads to a statistically different solution. This conclusion is not surprising, considering the existence of an inverse energy cascade in 2-D turbulence, which implies that the high-wavenumber Fourier modes remain active and affect the evolution of the low-wavenumber modes. The implication of this behavior has not been implemented in turbulence models because there were not yet any alternative methods to replace gridpoint and Fourier representations.

In the same paper [62] we showed that there is a possible separability between active modes, namely the coherent structures corresponding to the strong wavelet packet coefficients, and passive modes, namely the vorticity filaments of the background flow corresponding to the weak wavelet packet coefficients. Both components are multiscale, which is why the Fourier representation is not able to disentangle them and *a fortiori* to model them. According to Weiss analysis [158] the coherent structures correspond to elliptic regions (nearby fluid trajectories remain nearby) where rotation ω^2 dominates strain σ^2, while the background flow corresponds to hyperbolic regions (nearby fluid trajectories separate exponentially) where strain σ^2 dominates rotation ω^2. In the very small scales, for elliptic regions the local Reynolds number $\tilde{\mathrm{Re}}(\mathbf{x}, r)$ is larger than one, while for the hyperbolic regions it is smaller than one, which indicates that the only background flow is laminar and dissipative (Fig. 5). Coherent structures are local quasistationary solutions of Navier–Stokes equations. The probability distribution of the velocity field associated to the coherent structures is out of thermal equilibrium and varies depending on their configuration in space. On the contrary the background flow has already thermalized due to the very strong mixing resulting from the straining imposed by the coherent structures. Therefore the probability distribution of the velocity field of the background flow is stationary and no longer depends on the spatial configuration of the coherent structures. We should then be able to model this background flow by an *ad hoc* stochastic process having the same enstrophy and the same statistics, in particular the same spectral slope, whereas the coherent structures should be explicitly computed in phase space. A possible direction would be to construct a wavelet or wave packet frame (namely a quasi-orthogonal basis) made of local solutions of the linearized Navier–Stokes equations (namely any isotropic smooth function). We do not yet know neither to construct it, nor how to compute Navier–Stokes equations in it, but preliminary steps in this direction will be discussed in Section VI.

In an unpublished work [61] we have also shown that the presence of coherent structures inhibits the nonlinear instability of the background flow, namely the formation of new coherent structures. Using the wavelet packet representation to extract the coherent structures, we then computed the evolution of the remaining background flow in the absence of coherent structures, and observed the emergence of new ones out of it (Fig. 6). Actually when coherent structures are present, they impose a strain on the background flow which then inhibits the formation of new coherent structures. Due to this strain there is no energy or enstrophy backscatter from the incoherent to the coherent components of 2-D flows. The next step to validate this observation will be to compute the different transfers between coherent and incoherent structures components of the flow (namely from coherent structures to coherent structures, from coherent structures to background, from background to coherent structures, and from background to background) and check that there is no transfer from background to coherent structures. If this is confirmed, there will be a possible wavelet separability between the coherent and incoherent flow components and we may then be able to propose new parametrizations based on this gap.

B. Three-Dimensional Turbulence Modeling

The assumption that the high-wavenumber Fourier modes are slaved to the active low-wavenumber Fourier modes [158] is probably also wrong for 3-D turbulence due to the recent evidence of energy backscattering [44]–[46], [104], [135], i.e., inverse energy transfer from small to large scales, resulting from the presence of organized structures which locally interact and transfer energy to larger scales. We should take this observation with caution knowing that the amount of backscattering observed depends sensitively on the sharpness of the spectral filter used. There are two other reasons to explain why this assumption is not valid and should be revised.

The first reason comes from the fact that we do not have any universal theory of turbulence aside from the statistical theory which deals with homogeneous and isotropic ensemble averages, while a numerical simulation computes one flow realization at a time (at the highest resolution possible with present supercomputers) and not ensemble averages (which requires too many computations of the same turbulent flow). Actually, each flow realization is, unlike an ensemble average, highly inhomogeneous due

to the presence of coherent structures. As we have shown in performing wavelet analyses of 2-D and 3-D turbulent flows, coherent structures are multiscale and, through their mutual nonlinear interactions, are responsible for inverse energy transfers. If the computational grid is too coarse, its resolution is insufficient to accurately compute these transfers. Likewise subgrid-scale parametrization is only able to model direct transfers and inverse transfers in a statistical sense, assuming homogeneity, but not for the indivisual inhomogeneous flow realization one computes. In fact backscattering is a major unresolved drawback of current numerical methods, which will last as long as we will be unable to separate the coherent structures from the background flow and take into account the parametrization of homogeneous turbulent components separately from the inhomogeneous components.

The second reason comes from the fact that our current numerical methods are defined, either in grid-point, finite element, or Fourier representation, and are unable to compute multiscale objects with a small number of coefficients. This would be possible using either adapted multigrid or wavelet numerical methods. Multigrid techniques were proposed 20 years ago by Achi Brandt [27] for solving elliptic problems, such as the diffusion equation; they were then adapted to quasistationary problems, but do not yet seem optimal to solve time-dependent problems. Actually, the multigrid approach is very similar to a wavelet approach using a hat scaling function, which is very well localized in physical space and corresponds to a set of embedded grids, but which is too delocalized in spectral space and tends to produce large errors in the higher order derivatives of the solution. As far as we know, locally refined multigrid techniques have been tried for the Navier–Stokes equations, but not yet in the turbulent regime.

One possible approach is to use the wavelet Reynolds number to split the Navier–Stokes equations at each time step into advection and diffusion operators, which will be solved separately using the most appropriate numerical method and turbulence parameterization for each operator. Namely, the advection term is computed where $\tilde{\mathrm{Re}}(\mathbf{x}, r) > 1$, and the diffusion term where $\tilde{\mathrm{Re}}(\mathbf{x}, r) \leq 1$. This method makes sense only if the flow is represented either in a multigrid or in a wavelet representation (see Section VI). We could for instance built an appropriate wavelet frame (namely a quasi-orthogonal basis) made of local solutions of the linearized Navier–Stokes equations (same in this case as the heat equation), which could be any isotropic smooth function such as a circular Gaussian vortex (e.g., the Burger's vortex).

Actually, as we have already said, the Navier–Stokes equations are computationally intractable for the large Reynolds number limit which corresponds to fully developed turbulent flows. Although the use of wavelets may improve current numerical methods for solving the Navier–Stokes equations (see Section VI), a more promising direction may be to look for a new set of equations specific to the turbulent regime. Such equations would be written in terms of a small number of new variables corresponding to the degrees of freedom attached to the coherent structures. As a consequence they will break some of the symmetries of Navier–Stokes, in particular its translational invariance. This is analagous to the way in which Boltzmann's equation, describing the macroscopic level, breaks the time reversibility of Newton's equation, describing the microscopic level. For modeling turbulent flows we ought to go one step further in this hierarchy of embedded equations and define a new "organized" level emerging out of the thermalized background flow.

C. Stochastic Models

The idea is to find models of turbulence that mimic the behavior of Navier–Stokes equations at high Reynolds numbers, but which would be easier to solve numerically and perhaps even analytically. These models could then be used to study some properties of turbulent flows, such as energy cascade, probability distribution functions, intermittency, and departure from Kolmogorov's scaling.

The first attempt was done in 1974 by Desjanski and Novikov [42] who devised a so called *shell model* where the Navier–Stokes equations were represented on a discrete set of wavenumbers in Fourier space, each Fourier shell corresponding to one octave. The coupling between different octaves was supposed to be local in Fourier space and energy was transferred only from large to small scales. Such shell models, sometimes called *cascade models*, are still popular because with them it is easy to obtain very large inertial range, up to Reynolds numbers 10^{10}, at a limited computational cost. The number of degrees of freedom needed to compute 3-D Navier–Stokes equations by standard direct simulations scale as $\mathrm{Re}^{9/4}$, whereas it scales as Re for shell models. The weak point of shell models is that the vectorial structure of Navier–Stokes equations is lost, the incompressibility condition is not satisfied and they do not give accurate information on the spatial structure of the flow.

In 1981, Zimin [71], [163], [162] proposed another model, called the *hierarchical model*, defined in both space and scale. He projected the 3-D Navier–Stokes equations onto a Paley–Littlewood basis and dicretized them by octaves, considering a limited number of vortices for each octave, few in the large scales and more in the small scales in accordance to the uncertainty principle. He then assumed that each vortex is advected by the velocity field of the larger vortices, which lead him to propose a set of semi-Lagrangian wavelets to compute the flow evolution. This impressive work foreshadowed the wavelet decomposition, and has since been developed by Frick [69], [70], [6]. Hierarchical models are more physical than shell models because they also take into account the vortex motions, but they are still not very realistic from a physical standpoint because they neglect the vortex deformation which is responsible for energy transfers and subsequent dissipation. Recently Eyink [57], in an unpublished paper, criticized this approach by showing that semi-Lagrangian wavelets do not remove the effect of large-scale convection to the

energy transfers and therefore do not guarantee their locality (in wavenumber space). This is again due to Heisenberg's uncertainty principle and is related to the fact that it is impossible to compare transfers between wave numbers and transfers between wavelets, this point has already been discussed in Section IV.

Ideas on turbulence evolve at a very slow pace. As example of this, let us quote what Liepmann wrote in the *Proceedings of the Turbulence Conference* held in Marseille in 1961 [111].

> The success of the spectral representation of turbulent fields is due, after all, not to the belief in the existence of definite waves but to the possibility of representing quite general functions as Fourier integrals. In the application to stochastic problems the usefulness of the Fourier representation stems essentially from their translational invariance. Consequently, really successful models for representing turbulent shear flows will require far broader invariance considerations. It is clear that the essence of turbulent motion is vortex interaction. In the particular case of homogeneous isotropic turbulence this fact is largely masked, since the vorticity fluctuations appear as simple derivatives of the velocity fluctuations. In general this is not the case, and a Fourier representation is probably not the ultimate answer. The proposed detailed models of an eddy structure represent, I believe, a groping for an eventual representation of a stochastic rotational field, but none of the models proposed so far has proven useful except in the description of a single process.

These remarks, written 35 years ago, are still very pertinent and define the direction we should take for future research in turbulence.

Nowadays, using continuous wavelets we can construct more elaborate stochastic processes. As Liepmann has perceived we should be able to synthesize stochastic rotational fields, built from a set of randomly translated, rotated and dilated elementary vortices, which should have the same non-Gaussian statistics as those observed for two and 3-D turbulent flows. Recently Eliott and Majda [53], [54] have used wavelets to build a Gaussian, stationary and self-similar stochastic process for synthetizing turbulent velocities fields satisfying Taylor's hypothesis and displaying Kolmogorov's energy spectrum. Using these synthetic velocity fields they recover Richardson's law for scalar pair dispersion [55]. Their method may be useful to model the background flow which, contrary to coherent structures, does have Gaussian statistics.

VI. Turbulence Computation

A. Direct Numerical Simulations

The numerical simulation of turbulent flows, based on the direct integration of the Navier–Stokes equations at high Reynolds number, requires a very large number of degrees of freedom which increases like Re in two dimensions and like $\mathrm{Re}^{9/4}$ in three dimensions. Among the numerous Eulerian and Lagrangian numerical schemes, one may identify two different points of view: the spectral and the physical ones. Historically the most important for fundamental studies, the spectral point of view is based on the scale invariance of the Euler equations which leads to the cascade concept; indeed, the vorticity (1) creates more and more scales of motion from the injection scales, linked to external force $\mathbf{F}$, to the dissipation scales, which are inversely proportional to the Reynolds number, and eventually generates a continuous Fourier spectrum. The first long-time simulations of 2-D turbulent flows [12], [112], [20] based on spectral methods, i.e., Fourier decomposition, could not attain realistic Reynolds numbers, because their resolution was not exceeding 512^2. On the other hand, the physical point of view relies on the visual analysis of numerical and laboratory experiments, which lead to the recognition of the important dynamical role played by the coherent structures. This resulted in the development of Lagrangian methods ([1], e.g., vortex methods [108] or contour dynamics methods [102]) which follow the motion of each vortex, but which are imprecise concerning the background flow between the vortices. Finite element or finite difference methods allow mesh refinement in regions of the flow where small structures appear, for instance in the boundary layer of an obstacle; unfortunately, automatic adaptive refinements requires postprocessing to follow these small structures.

Wavelet bases, in the context of PDE's numerical simulation, appear to be a good compromise between spectral methods (precise, but expensive), vortex methods (which automatically follow coherent structures, but not the background flow), and finite element or finite difference methods (local in space, but not precise). Wavelet numerical methods have already been used to solve Burgers' equation in 1-D [7], [83], and 2-D [23], Stokes' equation in 2-D [153], Kuramoto–Sivashinsky equation [126], Benjamin–Davis–Ono–Burgers' equation [68], the heat equation in 2-D [36], some flame equation in 1-D and 2-D [75], the nonlinear Schrödinger equation [79], Euler's equation [138], and Navier–Stokes' equation in 2-D [37], [77].

B. Wavelet Based Numerical Schemes

The localization of wavelet bases, both in space and scale, leads to an effective nonlinear compression of the solution as well as a sparse representation of the operators involved in (1). This can be justified by theoretical results and verified by numerical experiments.

The sparsity of the wavelet expansion of a given function is linked to its local smoothness: where the function is regular, the corresponding wavelet coefficients decrease with scale. This fact is related to the characterization of pointwise Hölder spaces [87], [84], and is illustrated in Fig. 3 in the *Mathematical Background* in this issue. Recall that for Fourier decomposition, the decay of the coefficients depends on the global regularity of the function [157]. Another important property of wavelets is given by the nonlinear approximation of functions: the approximation error between a function and its wavelet series taken as the

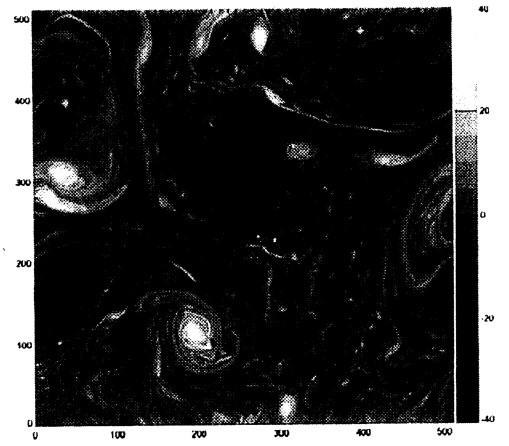

(a)

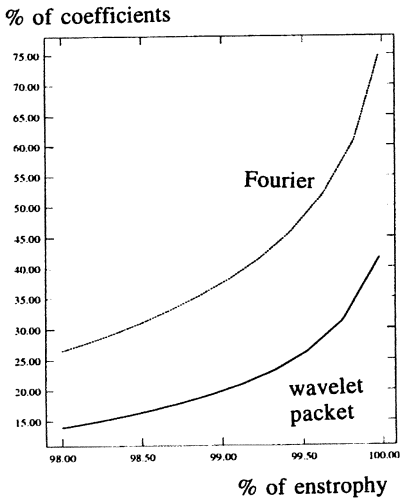

(b)

Fig. 7. Nonlinear compression of a vorticity field in Fourier basis versus compression in a wavelet packet basis. (a) Vorticity field computed with a resolution of 128^2. (b) Nonlinear compression in Fourier basis (dotted line) and in wavelet packet basis (dashed line).

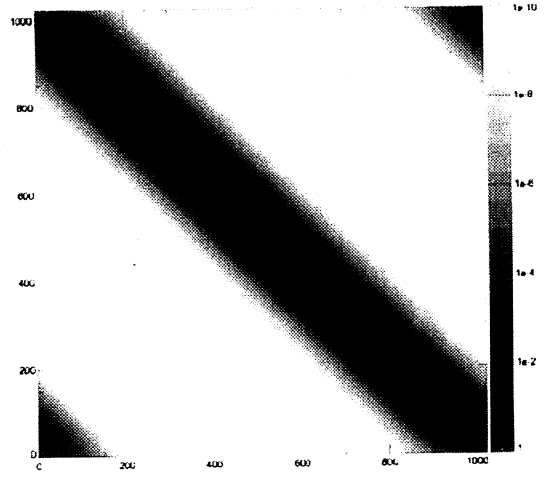

(a)

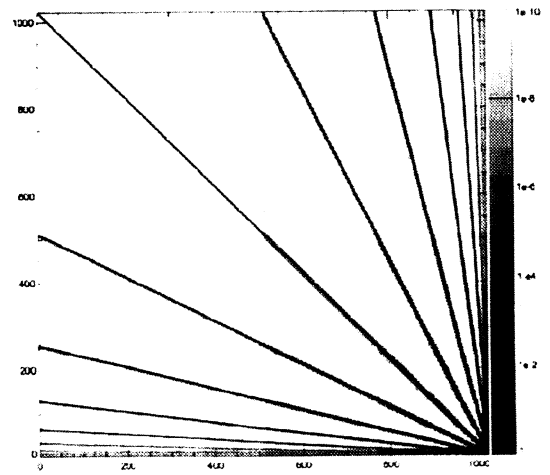

(b)

Fig. 8. Discretization matrix of the heat operator $(1-10^{-4}\nabla^2)^{-1}$. The gray code is a logarithmic scale from white to black, the significant values being black. (a) In finite differences of fourth order. (b) In a wavelet basis with the same precision.

N largest coefficients (in a given norm) can be estimated, in some Lebesgue space, by a (negative) power of N which depends on the smoothness or nonsmoothness of this function. This result follows from the characterization of Sobolev and Besov spaces by mean of wavelet coefficients [119], [43], [47]. Note that the nonlinear wavelet approximation of a given function is associated with a grid in physical space which is refined where there are singularities of this function [76].

A comparison of Fourier versus wavelet and wavelet packet nonlinear compression for a numerical vorticity field is shown on Fig. 7. We observe that the wavelet packet compression is more efficient and that the nonlinear wavelet compression is better behaved than the nonlinear Fourier one.

Another important consequence of the double localization (in space and scale) of wavelet bases is that some pseudo-differential operators become almost diagonal when decomposed into these bases. This is the case for the gradient operators and the heat kernel (decomposition of Calderon–Zygmund operators [119]). As an example the discretized heat kernel (on a 1024^2 grid) is projected onto a wavelet basis (Fig. 8(b)) and we observe that only 9.5% of the coefficients are greater than 10^{-8}, absolute value to be compared to the largest eigenvalue which is order one, instead of 21% for a finite difference projection (Fig. 8(a)).

These two fundamental properties (field compression and operator compression) allow us to define adaptive wavelet-based numerical schemes for solving PDE's. By neglecting small coefficients in the solution and/or in the operator's wavelet representation, each step of the algorithm is based on approximate but fast matrix-vector products computed in wavelet space. Note that the schemes based on scaling functions (often deliberately confused with wavelets) [81], [99], [68] instead of wavelet functions are no more efficient than classical finite element methods on a regular grid! Theoretical error and stability estimates for some particular wavelet schemes may also be derived [22], [40], [24].

C. Solving Navier–Stokes Equations in Wavelet Bases

The first wavelet adaptive schemes for the Navier–Stokes equations were derived by Charton [35] and Fröhlich and Schneider [77]. An equivalent scaling function scheme for solving the Euler equations has already been developed by Qian and Weiss [138]. Many approaches can be used to solve the 2-D Navier–Stokes equations. We will focus on the most developed (because the most commonly used) wavelet methods for solving PDE's: the Galerkin and Petrov–Galerkin schemes based on the discrete wavelet transform. Another way would be to develop Lagrangian-type wavelet methods, based on the continuous wavelet transform. An example is the traveling wavelet method [11] in which wavelets behave like particles evolving in phase-space coordinates.

The traveling wavelet method looks for an approximate solution of the above (51) which is a finite sum of wavelets evolving in phase-space

$$\omega(x,t) \approx \sum_{i=1}^{N} c_i(t)\psi\left(\frac{x-b_i(t)}{a_i(t)}\right), \quad a_i > 0 \tag{50}$$

where ψ is the base-wavelet and c_i, a_i, b_i, are respectively the time dependent amplitude, scale, and position parameters.

This method works well for linear equations such as the convection-diffusion equation, the Korteveg–deVries equation, and very recently was applied to the study of the formation of galaxies [18]. However, in the nonlinear case, the method encounters technical difficulties, which have not yet been completly overcome: these difficulties happen when two wavelets approach each other in phase space. This effect is also called "atom's collision."

Now, let us consider the 2-D Navier–Stokes equations written in terms of vorticity and stream function

$$\begin{cases} \frac{\partial \omega}{\partial t} + \mathbf{v}\cdot\nabla\omega = \nu\nabla^2\omega + f, & x \in [0,1]^2, \quad t > 0 \\ \nabla^2\Psi = \omega, \quad \mathbf{v} = (\frac{\partial \Psi}{\partial_y}, -\frac{\partial \Psi}{\partial_x}) \end{cases} \tag{51}$$

ω = voricity, $\mathbf{v}$ =, velocity, ∇ = kinematic viscosity, f = external force, and Ψ = stream funcion and periodic or Dirichlet or Neumann boundary conditions.

By introducing a time step δt and a classical semi-implicit time discretization and setting $\omega^n(x) \approx \omega(x, n\delta t)$ to be the approximate solution at time $n\delta t$, (51) is replaced, for example (we take here the simpliest but instable time scheme for sake of clarity) by

$$\begin{cases} (1-\nu\delta t\nabla^2)\omega^{n+1} = \omega^n + \delta t(f^n - v^n\cdot\nabla\omega^n) \\ \nabla^2\Psi^{n+1} = \omega^{n+1}, \quad v^{n+1} = \partial_y\Psi^{n+1}, -\partial_x\Psi^{n+1} \end{cases} \tag{52}$$

The spatial discretization is then performed by approximating, at time $n\delta t$, ω^n by a function ω_J^n belonging to a finite dimensional subspace V_J obtained from a multiresolution analysis $(V_j)_{j\geq 0}$ of the space $L^2([0,1]^2)$ (see the Mathematical Background). This spatial approximation can be of collocation type, i.e., grid point values or of Galerkin type, i.e., a projection onto a basis. The transformation between collocation and Galerkin representations uses an orthogonal wavelet transform. However, problems arise with adaptive schemes because it is difficult to take advantage of the sparsity of the wavelet decomposition, when going back and forth from gridpoints to wavelet representations. Let us be more precise and consider the 1-D case. Suppose that $\dim V_J = 2^J$. Then the function ω_J^n can be expanded onto the scaling function basis $(\varphi_{J,k})_{k=0,2^J-1}$ of V_J

$$\omega_J^n(x) = \sum_{k=0}^{2^J-1} c_{J,k}^n\,\varphi_{J,k}(x) \tag{53}$$

or onto a wavelet basis $(\psi_{j,k})_{0\leq j\leq J, k=0,2^j-1}$ of V_J

$$\omega_J^n(x) = \sum_{j=0}^{J-1}\sum_{k=0}^{2^j-1} d_{j,k}^n\,\psi_{j,k}(x) + c_{0,0}^n. \tag{54}$$

In the collocation method, the function ω_J^n is naturally associated with a regular grid $(x_k = k2^{-J})_{k=0,2^J-1}$ of [0, 1] and its corresponding collocation values $\omega_J^n(x_k)$. Often, by using properties of scaling functions $\varphi_{J,k}$ one can identify

$$\omega_J^n(x_k) \approx 2^{-J}c_{J,k}^n. \tag{55}$$

The wavelet Galerkin method is based on the wavelet coefficients $d_{j,k}^n$, and in practice uses only the few (non-negligible) coefficients larger than a given threshold ε: $\{d_{j,k}^n; |d_{j,k}^n| > \varepsilon\}$. Mallat's fast wavelet algorithm works well for regular grids, but is no more efficient for irregular grids composed with the irregular grid points x_k corresponding to the "centers" of wavelets $\psi_{j,k}$, for which the coefficients of $\omega_J^n(x_k)$ satisfy $|d_{j,k}^n| > \varepsilon$.

To avoid the problem, one can introduce, when it exists, an interpolating function of V_J and adapt Mallat's fast wavelet algorithm [76]. Another way is to directly contruct interpolating scaling functions $\varphi_{J,k}$ and the corresponding interpolating wavelet basis $\psi_{j,k}$ [23], which avoids the problem. Last, one can construct an adaptive multiresolution analysis [137], but the algorithm is not yet effective.

The algorithm (52) for solving the 2-D Navier–Stokes equations can now be split into four steps which we will then discuss: 1) time stepping the heat equation, 2) solving a Poisson equation, 3) computing the nonlinear term, and 4) imposing the boundary conditions.

1) The Heat Equation Solution: Let us consider the discretised heat equation

$$(1-\nu\delta t\nabla^2)\omega^{n+1} = \omega^n + \delta t f^n. \tag{56}$$

The biorthogonal approach introduced in [110], [101], [76] consists of building a biorthogonal system from a classical wavelet basis $\psi_{j,k}$ setting first,

$$\theta_{j,k} = (1-\nu\delta t\nabla^2)^{-1}\psi_{j,k} \tag{57}$$

with suitable hypotheses on ψ. Then a system $\tilde{\theta}_{j,k}$ biorthogonal to $\theta_{j,k}$ is constructed, and (56) is reduced to the change of bases

$$\langle \omega^{n+1} \mid \psi_{j,k}\rangle = \langle \omega^n \mid \theta_{j,k}\rangle + \delta t\langle f^n \mid \theta_{j,k}\rangle \tag{58}$$

where the notation $\langle | \rangle$ means scalar product. This approach avoids inverting the operator and is simply a collocation problem, as we must return to grid values at each time step.

The Galerkin approach is to project (56) onto a classical, orthogonal, or biorthogonal wavelet basis $(\psi_{j,k})$ of the space V_J. We can write

$$\left(\langle \omega_J^{n+1} \mid \psi_{j,k} \rangle\right)_{j,k} = \mathrm{K}\left(\langle \omega_J^n + \delta t f \mid \psi_{j,k} \rangle\right)_{j,k} \quad (59)$$

where

$$\mathrm{K}_{(j,k),(j',k')} = \langle (1 - \nu \delta t \nabla^2)^{-1} \psi_{j,k} \mid \psi_{j',k'} \rangle \quad (60)$$

is the heat kernel, which is almost diagonal, as explained in Section VI-B, Fig. 8(b). This step is based on approximated but fast matrix-vector products. An easy way to reduce the previous 2-D system to several 1-D systems is to use a tensor wavelet basis $(\psi_{j,k}(x) \cdot \psi_{j',k'}(y))$ and to split the 2-D heat kernel into two one-dimensional operators

$$(1 - \nu \delta t \nabla^2)^{-1} \approx \left(1 - \nu \delta t \frac{\partial^2}{\partial x^2}\right)^{-1} \left(1 - \nu \delta t \frac{\partial^2}{\partial y^2}\right)^{-1} \quad (61)$$

as in the alternating direction implicit (ADI) method [36], [37].

2) The Poisson Equation: The solution to the Poisson equation

$$\nabla^2 \Psi^{n+1} = \omega^{n+1} \quad (62)$$

can be obtained as the steady state solution of the heat equation, which, as in ADI methods, is reached in only a few iterations by considering iterated powers K^n of the heat kernel K (60) which become sparser with n [36].

An alternative approach, proposed by Jaffard [87], is to consider the well-conditioned system

$$\mathrm{PAPP}^{-1}\left(\langle \Psi_J^{n+1} \mid \psi_{j,k} \rangle\right)_{(j,k)} = \mathrm{P}\left(\langle \omega_J^{n+1} \mid \psi_{j,k} \rangle\right)_{(j,k)} \quad (63)$$

where A is the Galerkin matrix of the Laplacian in a wavelet basis: $\mathrm{A}_{(j,k),(j',k')} = \langle \nabla^2 \psi_{j,k} | \psi_{j',k'} \rangle$ and P is the diagonal preconditioning matrix: $\mathrm{P}_{(j,k),(j',k')} = 2^{-j} \delta_{j,j'} \delta_{k,k'}$, in 1-D (in 2-D this should be modified according to the chosen 2-D wavelet basis). Jaffard proved that the condition number of PAP does not depend on the order of the system. Then the solution of (63) can be reached in a few iterations by a classical conjugate gradient method.

3) The Nonlinear Term: The nonlinear term $\mathbf{v}^n \cdot \nabla \omega^n$ can be computed either by a collocation or by a Galerkin method. The collocation (also called pseudo-spectral) method can be sketched as follows: starting from the wavelet coefficients of $\mathbf{v}^n$ and ω^n, compute the wavelet coefficients of $\nabla \omega^n$. Then, through an inverse wavelet transform, obtain the grid point values of $\mathbf{v}^n$ and $\nabla \omega^n$ on the associated grid, as above. Then the products are calculated at each grid point, and finally the wavelet coefficients of the nonlinear term are obtained through a direct wavelet transform. This collocation method requires a fast wavelet transform between grid points and sparse coefficients sets. This problem was edvocated in the previous Section VI-C. Recently, Fröhlich and Schneider [76] have developed a wavelet transform for lacunary bases.

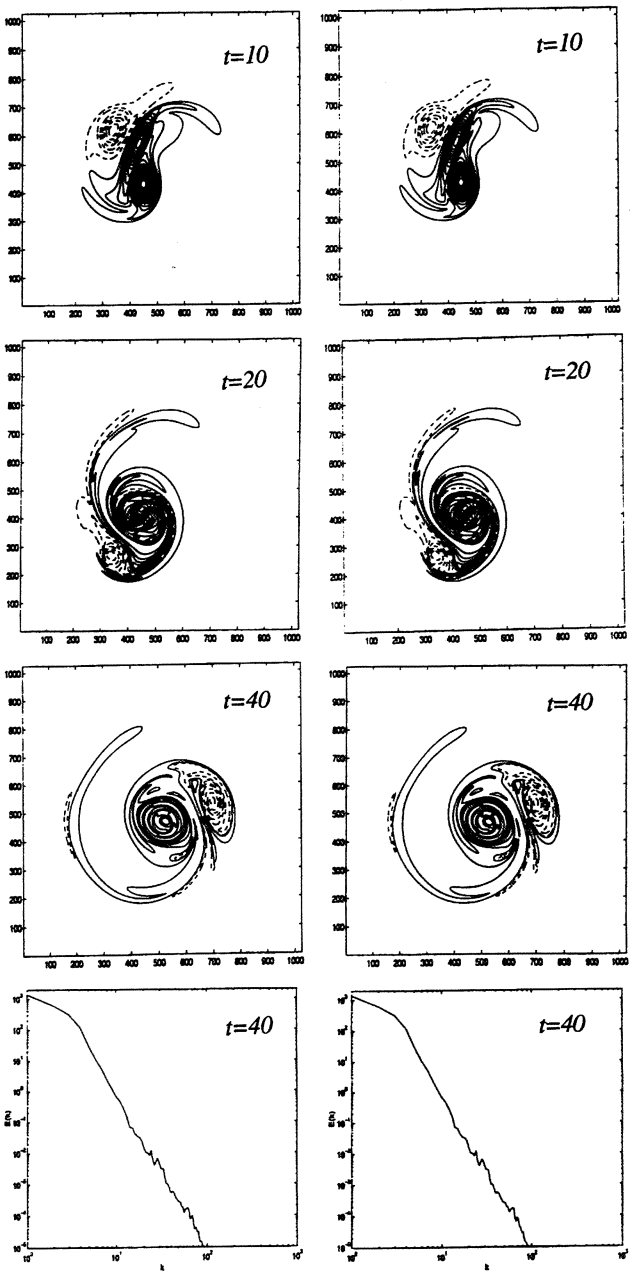

Fig. 9. Comparison of a pseudo-spectral and a pseudo-wavelet computation of 2-D Navier–Stokes equations (this computation was done in collaboration with Philippe Charton). (a) Vorticity evolution from $t = 10$ to $t = 40$ and the energy spectrum at $t = 40$ computed with a pseudo-spectral code. (b) Vorticity evolution from $t = 10$ to $t = 40$ and the energy spectrum at $t = 40$ computed with a pseudo-wavelet code.

On the other hand, a Galerkin method works only in the wavelet coefficient space, avoiding transforms between physical and wavelet space. The nonlinear term is then written as convolutions between the wavelet coefficients of $\mathbf{v}^n$ and $\nabla \omega^n$; these convolutions involve triple wavelet connection coefficients of the form $\langle \psi_{j_1,k_1} \psi'_{j_2,k_2} \mid \psi_{j_3,k_3} \rangle$. *A priori* the complexity of such a calculation is very large, but the method can be competitive for two reasons. 1) Since the wavelets are localized both in space and scale, connec-

tion coefficients vanish when two of the three wavelets are separated either in scale or space. Hence, only a limited small number of terms remains in the convolution. 2) The method can, more easily than collocation, handle adaptive description of the fields, i.e., the convolution can be restricted to only the significant components of the flow [133].

4) The Boundary Conditions: Boundary conditions are in general included in the definition of the spaces $(V_j)_{j\in Z}$ when constructing the multiresolution analysis. The simplest and most popular (due to the development of Fourier spectral methods) are periodic boundary conditions for which periodic wavelets, in one or several dimensions, can be easily constructed [131]. For Dirichlet or Neumann boundary conditions, compactly supported bases have recently been constructed in 1-D [38], [123], [124], and these bases are also associated to fast orthogonal wavelet transforms, like for the periodic case. They can easily be included in the previous algorithms, since the extension to cubic domains in several dimensions is trivial using tensor products of wavelets (in practice all 2-D orthogonal wavelet bases are tensor products, which raises the problem of anisotropy).

One should also mention the existence of divergence-free wavelet bases [106], [105], which can be used for the velocity-pressure formulation of Navier–Stokes (1) and automatically take into account the incompressibility condition [153].

Charton [35] has recently developed a code for solving 2-D periodic Navier–Stokes equations. It uses a "pseudo-wavelet" (by comparison with pseudo-spectral) method. The time discretization is a second order semi-implicit scheme and the space discretization is performed by a fourth order wavelet approximation. As explained in (59)–(61), the algorithm is based on a splitting of the 2-D heat kernel, associated to a tensor product wavelet basis. The Poisson solution is given by the steady state solution of the heat equation. All these steps use the lacunarity of the wavelet representation for the operators and for the solution. The nonlinear term is computed by a collocation method on a regular grid, and this point should be improved.

The first results at low resolution (128^2) are shown on Fig. 9. This work is actually in progress, the lastest tests validate the method by comparison with a pseudo-spectral code. Note that a global simulation at resolution 1024^2 can be run on a workstation.

VII. Conclusion

The main factor limiting our understanding of turbulent flows is that we have not yet identified the structures responsible for its chaotic and therefore unpredictible behavior. Based on laboratory and numerical experiments, we think that vortices (or coherent structures) are these elementary objects, from which we may be able to construct a new statistical mechanics and define equations appropriate for computing fully developed turbulent flows.

The quasi-singular vortices encountered in turbulent flows are, by their nature, very rare. In fact, the Cafarelli–Kohn–Nirenberg theorem shows that singular structures, if they exist, must be of Hausdorf measure zero in space and time. The present statistical diagnostics are low order and thus insensitive to rare events, i.e., coherent structure, because their effect appears only in the higher order statistics. An example of this is the fact that the low order structure functions follow Kolmogorov's law (which assumes a homogeneous structureless and nonintermittent flow), while the higher order structure functions depart strongly from this law (because turbulent flows are actually highly intermittent). To efficiently analyze the coherent structures of turbulence one requires either a high order statistical method or some conditional averaging.

Using a wavelet representation instead of a Fourier representation minimizes the restrictions on the basis functions, enlarging them to Sobolev, Hölder, and Besov spaces. Moreover, the Fourier basis used by the present statistical theory of turbulence is not the appropriate functional representation space for analyzing the physical structure of a flow because it averages over space and thus loses all spatial information. Furthermore, the Fourier energy spectrum is sensitive to only the strongest isolated singularity in the flow, and even then can give no information about the form or location of this singularity. In short, Fourier space analysis is unable to disentangle coherent structures from the rest of the flow.

The complementary simultaneous space and scale information provided by the wavelet representation makes it an appropriate tool for identifying and analyzing coherent structures in turbulent flows. The wavelet transform can be used to segment the vorticity field into coherent and incoherent components as the first stage in a conditional sampling algorithm. Such a segmentation method respects Galilean invariance because it is performed on the vorticity field and not on the velocity field, which loses Galilean invariance. A local wavelet analysis can also give the strength and form of any quasi-singular isolated structures, which correspond to the coherent components, and separate them from the background flow, which corresponds to the incoherent components.

Different wavelet techniques must be used depending on whether the flow contains oscillating (e.g., spiral) or nonoscillating (e.g., cusp) type singularities, and whether it contains isolated (e.g., a single cusp or spiral) or dense (e.g., fractal) distributions of singularities. For example, the current wavelet-based methods for determining the singularity spectrum of a multifractal work only if the signal does not contain oscillating singularities. Turbulence may contain both types of singularities in either dense or isolated distributions. It is therefore important to determine from the beginning whether a given turbulence signal contains oscillating singularities and how these singularities are distributed. This classification is possible using a wavelet-based diagnostic.

In Section III-E we reviewed the wavelet-based methods for detecting and analyzing the singular structure of a signal. We saw that these methods are useful, not only because they provide new information which cannot be obtained using other methods, but also because they formally

unify a wide range of previously disparate approaches. For instance the wavelet-based method of calculating the structure functions unifies their analysis with the calculation of energy spectra and the strength of local singularities. Furthermore, wavelets play the role of "generalized boxes" in a new form of the standard box-counting algorithm used to estimate fractal dimensions. This algorithm brings out the intimate relationship between structure functions and multifractals. The application of these methods to turbulence is still in its first stages, although they have already produced interesting and stimulating new results.

In Section IV we showed that wavelet analysis has been an essential tool for identifying coherent structures as phase-space regions correlated in both space and scale, and for studying their scaling properties. Wavelet analysis has helped to relate the intermittency of turbulent flows to the presence of organized coherent structures, and explained why the predictions of the statistical theory of turbulence are not verified for high-order statistics. The wavelet representation may also be used to compute the transfers of energy and of enstrophy between coherent and incoherent components of turbulent flows.

In Section V we reviewed several applications of wavelets and wavelet packets to turbulence modeling. In particular, we showed that the wavelet packet representation, associated with a maximum entropy statistical method and a nonlinear filtering procedure, extracts the coherent structures in a computationally efficient way. Turbulent motions are nonseparable in the Fourier representation, while a wavelet representation may be able to provide such separability. We have reasons to expect a gap in wavelet coordinates between organized structures to be explicitly computed and random background flow to be modeled by an appropriate stochastic process. This decomposition may be the basis for a new way of numerically simulating turbulent flows and possibly other kind of intermittent behaviors having similar statistics.

In Section VI we summarized the progresses that has been made in actually computing partial differential equations in wavelet space. Numerous promising experiments have been carried out using wavelets on Burgers' equation in 1-D or 2-D, heat equation or Stokes equation in 2-D and Navier–Stokes equations in 2-D. All these experiments have shown that wavelet approaches are valid and sometimes superior to existing numerical methods.

In conclusion, we think that the wavelet functional representation may be the proper tool for building a statistical mechanics of turbulence based on the identification of elementary dynamical structures from the observational data we have. This theory will replace the present Fourier-space statistical theory of turbulence which is based on the symmetries of the Navier–Stokes equations. We are now convinced that Navier–Stokes equations are not the appropriate model equations to compute large Reynolds flows. Indeed in this limit, there is probably some symmetry breaking associated with the production of coherent structures out of the random background flow. This is precisely the difference between a statistical theory and a statistical mechanics!

Turbulence research is a kind of tragicomedy—tragic due to its military (atomic bomb, missiles, reentry vehicles) applications—and comic because at each generation we seem fated to rediscover old ideas. For instance, our understanding of dissipation and turbulence modeling is the same as what Richardson was suggesting when he wrote: "Diffusion is a compensation for neglect of detail. By anarbitrary choice we try to divide motions into two classes: (a) Those which we treat in detail. (b) Those which we smooth away by some process of averaging," [142] and the program we develop corresponds to the prescription for turbulence research proposed 47 years ago by Dryden when he wrote:

> It is necessary to separate the random processes from the nonrandom element [49].

Wavelets, as a new mathematical tool, will certainly bring new insights to assert present methods and hopefully to help understanding turbulent flows. But knowing the past difficulties encountered in this field, we should not be too optimistic, nor should we oversell wavelets. As Sadourny, director of our laboratory, likes to say quite ironically:

> "Wavelets? You mean this new approach which will waste another 20 years of turbulence research!"

ACKNOWLEDGMENT

The authors thank Philippe Charton, Echeyde Cubillo, and Thierry Philipovitch who computed some tof the results presented here. The authors also thank Aimé Fournier, Alain Arnéodo, Claude Bardos, Claude Basdevant, Achi Brandt, Gregory Eyink, Patrick Flandrin, Peter Frick, Stéphane Jaffard, Abdelhaq Hamza, Stéphane Mallat, Keith Moffatt, Basil Nicolaenko, Robert Sadourny, Kai Schneider, Bruno Torresani, Suzanne Tourville, Laurette Tuckerman, Christos Vassilicos, and Victor Wickerhauser for reading this paper and making useful comments on it. M. Farge is grateful to Dr. Coulombier for lending his house in Brittany in July 1995 to write this paper in a quiet atmosphere.

REFERENCES

[1] R. Abgrall and C. Basdevant, "Un schéma numérique semi-Lagrangien pour la turbulence bidimensionelle," *C. R. Acad. Sci. Paris*, t. 305, série I, pp. 315–318, 1987.

[2] P. Abry, S. Fauve, P. Flandrin, and C. Laroche, "Analysis of pressure fluctuations in swirling turbulent flows," *J. de Physique II*, vol. 4, pp. 725–733, 1994.

[3] F. Anselmet, Y. Gagne, E. J. Hopfinger, and R. A. Antonia, "High-order velocity structure function in turbulent shear flows," *J. Fluid Mech.*, vol. 140, pp. 63–89, 1984.

[4] A. Arnéodo, E. Bacry, and J. F. Muzy, "The thermodynamics of fractals revisited with wavelets," *Physica A.*, vol. 213, pp. 232–275, 1995.

[5] ——, "Oscillating singularities in locally self-similar functions," to be published.

[6] E. Aurell, P. Frick, and V. Shaidurov, "Hierarchical tree-model of 2D-turbulence," *Physica D.*, vol. 72, pp. 95–109, 1994.

[7] E. Bacry, S. Mallat, and G. Papanicolaou, "A wavelet based space-time adaptive numerical method for partial differential equations," *Math. Mod. Num. Anal.*, vol. 26, p. 793, 1992.

[8] R. Balian, "Un principe d'incertitude fort en thorie du signal ou en mécanique quantique," *C. R. Acad. Sci. Paris*, vol. 292, II, pp. 1357–1361, 1981.

[9] C. Bardos, F. Golse, and D. Levermore, "Fluid dynamical limit of kinetic equations: 1. formal derivations," *J. Stat. Phys.*, vol. 63, pp. 323–344, 1991.
[10] ——, "Fluid dynamical limit of kinetic equations: II. convergence proofs for the Boltzmann equation," *Com. Pure Appl. Math.*, vol. 46, no. 5, pp. 667–754, 1993.
[11] C. Basdevant, M. Holschneider, and V. Perrier, "Méthode des ondelettes mobiles," *C. R. Acad. Sci. Paris*, série I, t. 310, pp. 647–652, 1990.
[12] C. Basdevant, B. Legras, R. Sadourny, and M. Béland, "A study of barotropic model flows: Intermittency waves and predictability," *J. Atmos. Sci.*, vol. 38, pp. 2305–2326, 1981.
[13] G. K. Batchelor, "Computation of the energy spectrum in homogeneous two-dimensional turbulence," *Phys. Fluid, suppl. II*, vol. 12, pp. 233–239, 1969.
[14] ——, *Homogeneous Turbulence*. Cambridge, UK: Cambridge Univ. Press, 1953.
[15] G. K. Batchelor and A. A. Townsend, "The nature of turbulent motion at large wave numbers," in *Proc. Royal Soc. A*, 1949, vol. 199, pp. 238–255.
[16] G. Battimelli, "The mathematician and the engineer: The statistical theories of turbulence in the 20's," *Riv. Stor. Sci.*, vol. 1, no. 1, pp. 73–94, 1984.
[17] G. Battle and P. Federbush, "Divergence-free vector wavelets," *Michigan Math. J.*, vol. 40, pp. 181–195, 1993.
[18] N. Benhamidouche, "Ondelettes mobiles et l'instabilité gravitationnelle," Ph.D. dissertation, Université d'Aix-Marseille II, 1995.
[19] R. Benzi *et al.*, "Extended self-similarity in the dissipation range of fully developed turbulence," *Europe. Phys. Lett.*, vol. 24, no. 4, pp. 275–279, 1993.
[20] R. Benzi, G. Paladin, G. Parisi, and A. Vulpiani, "Power spectra in two-dimensional turbulence," *J. Phys. A*, 1984.
[21] G. Beylkin, "Wavelets, MRA and fast numerical algorithms," in *INRIA Lectures*, May 1991.
[22] G. Beylkin, R. Coifman, and V. Rokhlin, "Fast wavelet transforms and numerical algorithms I," *Comm. on Pure and Applied Math.*, vol. 43, pp. 141–183, 1991.
[23] S. Bertoluzza, "Adaptive wavelet collocation method for the solution of Burgers equation," *Transport Theory and Statistical Physics*, to be published,
[24] S. Bertoluzza, Y. Maday, and J. C. Ravel, "A dynamically adaptive wavelet method for solving partial differential equations," *Comput. Methods Appl. Mech. and Eng.*, vol. 116, pp. 293–299, 1994.
[25] S. Bertoluzza, G. Naldi, and J. C. Ravel, "Wavelet methods for the numerical solution of boundary value problems on the interval," in *Wavelets: Theory Algorithms and Applications*, C. K. Chui, L. Montefusco, and Puccio, Eds. New York: Academic, 1994.
[26] J. Boussinesq, "Essai sur la théorie des eaux courantes," *Mémoire de l'Acad. Sci. Paris*, vol. 23, no. 1, pp. 1–680, 1877.
[27] A. Brandt, "Multigrid techniques with applications to fluid dynamics: 1984 guide," *VKI Lecture Series*, pp. 1–176, 1984.
[28] O. Cadot, S. Douady, and Y. Couder, "Characterization of the low-pressure filaments in a three-dimensional shear flow," *Phys. Fluids*, vol. 7, no. 3, pp. 630–646, 1995.
[29] L. Cafarelli, R. Kohn, and L. Nirenberg, "Partial regularity of suitable weak solutions of the Navier–Stokes equations," *Comm. in Pure and Applied Math.*, vol. 35, pp. 771–831, 1982.
[30] E. Caglioti, P. L. Lions, C. Marchioro, and M. Pulvirenti, "A special case pf stationary flows for two-dimensional Euler equations: A statistical mechanics description," *Comm. Math. Phys.*, vol. 143, pp. 501–525, 1992.
[31] M. Cannone, *Ondelettes, Paraproduits et Navier-Stokes*. France: Diderot, 1995.
[32] B. Castaing, "Consequences d'un principe d'extremum en turbulence," *J. Physique*, vol. 59, pp. 147–156, 1989.
[33] B. Castaing, Y. Gagne, and E. Hopfinger, "Velocity probability density functions of high Reynolds number turbulence," *Physica D*, vol. 46, pp. 177–200, 1990.
[34] B. J. Cantwell, "Organized motion in turbulent flow," *Ann. Rev. Fluid Mech.*, vol. 13, pp. 457–515, 1981.
[35] P. Charton, "Produits de matrices rapides en bases d'ondelettes: Application à la résolution numérique d'équations aux dérivées partielles," Ph.D. dissertation, Université Paris 13, 1996.
[36] P. Charton and V. Perrier, "Factoriation sur bases d'ondelettes du noyau de la chaleur et algorithmes matriciels rapides associés," *C. R. Acad. Sci. Paris*, série I, t. 320, pp. 1013–1018, 1995.
[37] ——, "Toward a wavelet based algorithm for two dimensional Navier–Stokes equations," in *Proc. ICIAM 95*, 1995.
[38] A. Cohen, I. Daubechies, and P. Vial, "Wavelets on the interval and fast wavelet transforms," *Appl. Comp. Harm. Anal.*, vol. 1, pp. 157–188, 1993.
[39] Y. Couder, S. Douady, and O. Cadot, "Vorticity filaments," in *Turbulence: A Tentative Dictionary*, Tabeling and Cardoso, Eds. New York: Plenum NATO ASI Series, 1994.
[40] W. Dahmen, S. Prössdorf, and R. Schneider, "Multiscale methods for pseudo-differential equations on smooth closed manifolds," in *Wavelets: Theory Algorithms and Applications*, C. K. Chui, L. Montefusco, and Puccio, Eds. New York: Academic, 1994.
[41] A. Davis, A. Marshak, and W. Wiscombe, "Wavelet-based multifractal analysis of nonstationary and/or intermittent geophysical signals," in *Wavelet Transforms in Geophysics*, E. Foufoula-Georgiou and P. Kumar, Eds., pp. 249–298, 1994.
[42] V. Desnjanski and E. A. Novikov, "Model of cascade processes in turbulent flows," *Appl. Math. Mech.*, vol. 38, no. 3, pp. 507–513, 1974.
[43] R. DeVore, B. Jawerth, and V. Popov, "Compression of wavelet decomposition," *Amer. J. Mathemat.*, vol. 114, pp. 737–785, 1992.
[44] J. A. Domaradzki, "Nonlocal triad interactions and the dissipation range of isotropic turbulence," *Phys. Fluids A*, vol. 4, p. 2037, 1992.
[45] J. A. Domaradzki and R. S. Rogallo, "Local energy transfer and nonlocal interactions in homogeneous, isotropic turbulence," *Phys. Fluids A*, vol. 2, p. 413, 1990.
[46] J. A. Domaradzki, R. S. Rogallo, and A. A. Wray, "Interscale energy transfer in numerically simulated turbulence," *CTR, Proc. Summer Program*, 1990.
[47] D. Donoho, "Unconditionnal bases are optimal bases for data compression and statistical estimation," *Appl. Comp. Harmonic Anal.*, vol. 1, no. 1, pp. 100–115, 1993.
[48] T. Dupree, "Coarse-grain entropy in two-dimensional turbulence," *Phys. Fluid B4*, vol. 10, pp. 3101–3114, 1992.
[49] H. Dryden, "Recent advances in the mechanics of boundary layer flow," in *Advances in Applied Mechanics* New York: Academic, vol. 1, pp. 1–40, 1948.
[50] M. Duval–Destin and R. Murenzi, "Spatio-temporal wavelets: Application to the analysis of moving patterns," in *Progress in Wavelet Analysis and Applications*, Meyer and Roques, Ed. Paris: Editions Frontières, 1993, pp. 399–408.
[51] A. Einstein, "Méthode pour la détermination de valeurs statistiques d'observations concernant des grandeurs soumises à des fluctuations irrégulières," *Archive des Sciences Physiques et Naturelles*, vol. 37, pp. 254–255, 1914.
[52] D. Elhmaidi, A. Provenzale, and A. Babiano, "Elementary topology of two-dimensional turbulence from a Lagrangian viewpoint and single-particle dispersion," *J. Fluid Mech.*, vol. 257, pp. 533–558, 1993.
[53] F. W. Elliott and A. J. Majda, "A wavelet Monte-Carlo method for turbulent diffusion with many spatial scales," *J. Comput. Phys.*, vol. 113, no. 1, pp. 82–111, 1994.
[54] ——, "A new algorithm with plane waves and wavelets for random velocity fields with many spatial scales," *J. Comput. Phys.*, vol. 117, no. 1, pp. 146–162, 1995.
[55] ——, "Pair dispersion over an inertial range spanning many decades," to be published.
[56] G. L. Eyink and H. Spohn, "Negative-temperature states and large-scale, long-lived vortices in two-dimensional turbulence," *J. Statis. Phys.*, vol. 70, no. 3 and 4, pp. 833–887, 1993.
[57] G. L. Eyink, "Space-scale locality and semi-Lagrangian wavelets (energy dissipation without viscosity in ideal hydrodynamics)," preprint, Phys. Dept., Univ. Illinois at Urbana-Champain, 1995.
[58] M. Farge, "Wavelet transforms and their applications to turbulence," *Ann. Rev. Fluid Mech.*, vol. 24, pp. 395–457, 1992.
[59] ——, "The continuous wavelet transform of two-dimensional turbulent flows," in *Wavelets and Their Applications*, Ruskai *et al.*, Eds. New York: Jones and Bartlett, 1992, pp. 275–302.
[60] ——, "A wavelet Monte-Carlo method for turbulent diffusion with many spatial scales," *J. Comput. Phys.*, vol. 113, no. 1, pp. 82–111, 1994.
[61] M. Farge, E. Goirand, and N. Kevlahan, "Three coherent

structure interaction analyzed using wavelets packets," LMD Preprint, 1995.
[62] M. Farge *et al.*, "Improved predictability of two-dimensional turbulent flows using wavelet packet compression," *Fluid Dynam. Res.*, vol. 10, pp. 229–250, 1992.
[63] M. Farge, Y. Guezennec, C. M. Ho, and C. Meneveau, "Continuous wavelet analysis of coherent structures," *CTR, Proc. Summer Program*, 1990, pp. 331–348.
[64] M. Farge and M. Holschneider, "Interpretation of two-dimensional turbulence spectrum in terms of singularity in the vortex cores," *Europhys. Lett.*, vol. 15, no. 7, pp. 737–743, 1990.
[65] M. Farge, J. C. R. Hunt, and J. C. Vassilicos, *Wavelets, Fractals and Fourier Transforms*. New York: Clarendon, 1993.
[66] M. Farge and T. Philipovitch, "Coherent structure analysis and extraction using wavelets," in *Progress in Wavelet Analysis and Applications*, Y. Meyer and S. Roques, Eds. Paris: Editions Frontières, pp. 477–481, 1993.
[67] P. Federbush, "Navier and Stokes meet the wavelet," *Comm. Math. Phys.*, vol. 155, pp. 219–248, 1993.
[68] A. Fournier, "Wavelet representation of a lower atmospheric long nonlinear wave dynamics governed by the Benjamin-Davis-Ono-Burgers equation," in *Proc. SPIE: Wavelet Applicat. II*, H. H. Szu, Ed., 1995, vol. 2491, pp. 672–681.
[69] P. Frick, "Choix des ondelettes pour les modèles hiérarchiques de la turbulence," *Progress in Wavelet Analysis and Applications*, Y. Meyer and S. Roques, Eds. Paris: Editions Frontières, 1993, pp. 483–490.
[70] P. Frick, B. Dubrulle, and A. Babiano, "Scale invariance in a class of shell models," *The Phys. Rev. E*, vol. 51, no. 5, 1995.
[71] P. Frick and V. Zimin, "Hierarchical models of turbulence," *Wavelets, Fractals and Fourier Transforms*, Farge, Hunt, and Vassilicos, Eds. New York: Clarendon, 1993, pp. 265–283.
[72] U. Frisch and G. Parisi, *Turbulence and Predictability in Geophysical Fluid Dynamics and Climate Dynamics*, M. Ghil, R. Benzi, and G. Parisi, Eds. Amsterdam: North-Holland, 1985, p. 84.
[73] U. Frisch, P. L. Sulem, and M. Nelkin, "A simple dynamical model of intermittent fully developed turbulence," *J. Fluid Mech.*, vol. 87, pp. 719–736, 1978.
[74] U. Frisch and M. Vergassola, "A prediction of the multifractal model: The intermediate dissipation range," *Europhys. Lett.*, 1990.
[75] J. Fröhlich and K. Schneider, "An adaptive wavelet Galerkin algorithm for one and two-dimensional flame computation," *Europ. J. Mech. B/Fluids*, vol. 13, no. 4, pp. 439–471, 1995.
[76] ——, "An adaptive Wavelet-Vaguelette algorithm for the solution of nonlinear PDE's," *preprint*, Kaiserlautern Universität, 1995.
[77] ——, "Numerical simulation of decaying turbulence in an adaptive wavelet basis," *preprint*, Kaiserlautern Universität, 1995.
[78] Y. Gagne, "Etude expérimentale de l'intermittence et des singularités dans le plan complexe en turbulence dèveloppée," master's thesis, Université de Grenoble, France, 1987.
[79] L. Gagnon and J. M. Lua, "Symmetric Daubechies' wavelets and numerical solution of the nonlinear Schrödinger's equation," Tech. Rep., Lab. Nuclear Phys., Univ. Montreal, p. 16, 1994.
[80] A. D. Gilbert, "Spiral structures and spectra in 2-D turbulence," *J. Fluid Mech.*, vol. 193, pp. 475–497, 1988.
[81] R. Glowinski, W. M. Lawton, M. Ravachol, and E. Tenenbaum, "Wavelet solution of linear and nonlinear elliptic parabolic and hyperbolic problems in one space dimension," in *Proc. 9th Int. Conf. on Numerical Methods in Appl. Sci. and Engin.*, SIAM, Philadelphia, 1990.
[82] D. Gottlieb and S. A. Orszag, "Numerical analysis of spectral methods: Theory and applications," *Regional Conf. Series*, SIAM-CBMS, Philadelphia, 1977.
[83] A. Harten, "Adaptive multiresolution schemes for shock computations," *J. Comput. Phys.*, vol. 115, pp. 319–338, 1994.
[84] M. Holschneider and P. Tchamitchian, "Pointwise analysis of Riemann's 'nondifferentiable' function," *Inventiones Mathematicae*, vol. 105, pp. 157–176, 1991.
[85] J. C. R. Hunt and J. C. Vassilicos, "Kolmogorov's contributions to the physical and geometrical understanding of small-scale turbulence and recent developments," in *Proc. R. Soc. Lond. A*, 1991, vol. 434, pp. 183–210.
[86] S. Jaffard, "Some mathematical results about multifractal formalism for functions," in *Wavelets: Theory, Algorithms, and Applications*, C. K. Chui, L. Montefusco, and L. Puccio Eds., pp. 1–37, 1994.
[87] ——, "Wavelet methods for fast resolution of elliptic problems," *SIAM J. Numer. Anal.*, vol. 29, pp. 965–987, 1992.
[88] ——, "Pointwise smoothness, two-microlocalization and wavelet coefficients," *Publicacions Matematiques*, vol. 35, pp. 155–168, 1991.
[89] J. Jimenez, *The Role of Coherent Structures in Modeling Turbulence and Mixing*. New York: Springer, 1981.
[90] G. Joyce and D. Montgomery, "Negative temperature states for the two-dimensional guiding-center plasma," *J. Plasma Phys.*, vol. 10, p. 107, 1973.
[91] N. Kevlahan and J. C. Vassilicos, "The space and scale dependencies of the self-similar structure of turbulence," in *Proc. R. Soc. Lond. A.*, 1994, vol. 447, pp. 341–363.
[92] S. J. Kline, W. C. Reynolds, F. A. Schraub, and P. W. Rundstadler, "The structure of turbulent boundary layer," *J. Fluid Mech.*, vol. 30, p. 741, 1967.
[93] A. N. Kolmogorov, "The local structure of turbulence in incompressible viscous fluid for very large Reynolds numbers," *C. R. Acad. Sc. USSR*, vol. 30, pp. 301–305, 1941.
[94] ——, "On degeneration of isotropic turbulence in an incompressible viscous liquid," *C. R. Acad. Sc. USSR*, vol. 31, pp. 538–540, 1941.
[95] ——, "Dissipation of energy in the locally isotropic turbulence," *C. R. Acad. Sc. USSR*, vol. 32, pp. 16–18, 1941.
[96] ——, "A refinement of previous hypotheses concerning the local structure of turbulence in a viscous incompressible fluid at high Reynolds number," *J. Fluid Mech.*, vol. 13, pp. 82–85, 1962.
[97] R. H. Kraichnan, "Inertial ranges in two-dimensional turbulence," *Phys. Fluid*, vol. 10, pp. 1417–1423, 1967.
[98] R. H. Kraichnan and D. Montgomery, "Two-dimensional turbulence," *Reps. Progress in Physics*, vol. 45, p. 547, 1982.
[99] A. Latto and E. Tenenbaum, "Compactly supported wavelets and the numerical solution of Burger's equation," *C. R. Acad. Sci. Paris*, Série I, t. 311, pp. 903–909, 1990.
[100] S. Lazaar, J. Liandrat, and P. Tchamitchian, "Algorithme à base d'ondelettes pour la résolution numérique d'équations aux dérivées partielles à coefficients variables," *C. R. Acad. Sci. Paris*, Série I, t. 319, pp. 1101–1107, 1994.
[101] S. Lazaar, P. J. Ponenti, J. Liandrat, and P. Tchamitchian, "Wavelet algorithms for numerical resolution of partial differential equations," *Comput. Methods Appl. Mech. and Engrg.*, vol. 116, pp. 309–314, 1994.
[102] B. Legras and D. G. Dritschel, "A comparison of the contour surgery and pseudo-spectral methods," *J. Comput. Phys.*, vol. 104, no. 2, pp. 287–302, 1993.
[103] B. Legras, P. Santangelo, and R. Benzi, "High-resolution numerical experiments for forced two-dimensional turbulence," *Europhys. Lett.*, vol. 5, pp. 37–42, 1988.
[104] C. E. Leith, "Stochastic backscatter in a subgrid-scale model: Plane shear mixing layer," *Phys. Fluids*, vol. A, no. 3, pp. 297–299, 1990.
[105] P. G. Lemarié-Rieusset, "Un théorème d'inexistence pour les ondelettes vecteur à divergence nulles,"*CRAS Série I*, vol. 310, pp. 811–813, 1994.
[106] ——, "Analyses multirésolutions non orthogonales, commutation entre projecteur et derivation, et ondelettes à divergence nulle," *Revista Mat. Iberoamer.*, vol. 8, pp. 221–236, 1992.
[107] A. Leonard, *Adv. Geophys.*, vol. A 18, pp. 17, 1974.
[108] ——, "Vortex methods for flow simulation," *J. Comp. Phys.*, vol. 37, pp. 289–335, 1980.
[109] M. Lesieur, "New trends in large-eddy simulations of turbulence,"*Ann. Rev. Fluid Mech.*, vol. 28, pp. 45–82, 1996.
[110] J. Liandrat, V. Perrier, and P. Tchamitchian, "Numerical resolution of nonlinear partial differential equations using the wavelet approach," in *Wavelets and Their Applications*, Ruskai *et al.*, Eds. New York: Jones and Barlett, 1992, pp. 227–238.
[111] H. W. Liepmann, "Free turbulent flows," *Mécanique de la Turbulence*, Favre, Ed., pp. 211–227, 1962.
[112] J. C. McWilliams, "The emergence of isolated coherent vortices in turbulent flows," *J. Fluid Mech.*, vol. 146, pp. 21–43, 1984.
[113] Y. Maday, V. Perrier, and J. C. Ravel, "Adaptativité dynamique sur base d'ondelettes pour l'approximation d'équations aux dérivées partielles," *C. R. Acad. Sci. Paris*, Série I, t. 312, pp. 405–410, 1991.

[114] S. Mallat and W. H. Hwang, "Singularity detection and processing with wavelets," *IEEE Trans. Inform. Theory*, vol. 38, pp. 617–643, Mar. 1992.
[115] B. Mandelbrot, "Intermittent turbulence in self-similar cascades: Divergence of high moments and dimension of carrier," *J. Fluid Mech.*, vol. 62, pp. 331–358, 1975.
[116] C. Marchioro and M. Pulvirenti, *Mathematical Theory of Incompressible Nonviscous Fluids*. Berlin: Springer, 1994.
[117] M. Marion and R. Temam, "Nonlinear Galerkin methods," *SIAM J. Num. Anal.*, vol. 26, pp. 1139–1157, 1989.
[118] C. Meneveau, "Analysis of turbulence in the orthonormal wavelet representation," *J. Fluid Mech.*, vol. 232, pp. 469–520, 1991.
[119] Y. Meyer, *Ondelettes et Opérateurs*. Paris: Hermann, 1990.
[120] J. Miller, "Statistical mechanics of Euler equations in two dimensions," *Phys. Rev. Lett.*, vol. 65, no. 17, pp. 2137–2140, 1990.
[121] H. K. Moffatt, "Simple topological aspects of turbulent velocity dynamics," in *Proc. IUTAM Symp. on Turbulence and Chaotic Phenomena in Fluids*, T. Tatsumi, Ed. Amsterdam: Elsevier, 1984, p. 223.
[122] B. Mohammadi and O. Pirroneau, *Analysis of the k-ϵTurbulence Model*. Paris: Wiley–Masson, 1994.
[123] P. Monasse and V. Perrier, "Ondelettes sur l'intervalle pour la prise en compte de conditions aux limites," *C. R. Acad. Sci. Paris*, Série I, t. 321, pp. 1163–1169, 1995.
[124] ——, "Orthonormal wavelet bases adapted for partial differential equations with boundary conditions," mathematical preprints, Université Paris-Nord, no. 95-11, 1995.
[125] A. S. Monin and A. M. Yaglom, *Statistical Fluid Mechanics: Mechanics of Turbulence*. Cambridge, MA: MIT Press, 1975.
[126] M. Myers, P. Holmes, J. Elezgaray, and G. Berkooz, "Wavelet Projections of the Kuramoto–Sivashinsky equation I: Heteroclinic cycles and modulated waves for short systems," *Physica D*, vol. 86, pp. 396–427, 1995.
[127] A. M. Obukhov, "Energy distribution in the spectrum of a turbulent flow," *Izvestiya AN URSS*, vol. 4, pp. 453–466, 1941.
[128] L. Onsager, "The distribution of energy in turbulence," *Phys. Rev.*, vol. 68, p. 286, 1945.
[129] ——, "Statistical hydrodynamics," *Suppl. Nuovo Cimento*, suppl. vol. 6, pp. 279–287, 1949.
[130] G. Parisi and U. Frisch, "Fully developed turbulence and intermittency," *Turbulence and Predictability in Geophysical Fluid Dynamics and Climate Dynamics*, Ghil, Benzi, and Parisi, Eds. Amsterdam: North-Holland, 1985, pp. 71–88.
[131] V. Perrier and C. Basdevant, "Periodical wavelet analysis, a tool for inhomogeneous field investigation. Theory and algorithms," *Rech. Aérosp* no. 1989-3, 1989.
[132] V. Perrier, T. Philipovitch, and C. Basdevant, "Wavelet spectra compared to Fourier spectra," *J. Math. Phys.*, vol. 36, no. 3, pp. 1506–1519, 1995.
[133] V. Perrier and M. V. Wickerhauser, "Multiplication of short wavelet series using connection coefficients," preprint, 1995.
[134] T. Philipovitch, "Applications de la transformée en ondelettes continue à la turbulence homogène isotrope bidimensionelle," Ph.D. dissertation, *Université Paris VI*, 1994.
[135] U. Piomelli, W. H. Cabot, P. Moin, and S. Lee, "Subgrid-scale backscatter in transitional and turbulent flows," *CTR Proc. Summer Program*, 1990, pp. 19–30.
[136] A. M. Poliakov, "Conformal turbulence," *Nucl. Phys. B*, vol. 396, p. 367, 1993.
[137] P. Ponenti, "Algorithmes en ondelettes pour la résolution d'équations aux dérivées partielles," Ph.D. dissertation, Université d'Aix-Marseille I, 1994.
[138] S. Qian and J. Weiss, "Wavelets and the numerical solution of partial differential equations," *J. of Comp. Phys.*, vol. 106, pp. 155–175, 1993.
[139] O. Reynolds, "On the dynamical theory of incompressible viscous fluids and the determination of the criterion," in *Phil. Trans. Roy. Soc. London*, vol. 186, pp. 123–164, 1894.
[140] W. C. Reynolds, "Computation of turbulent flows," *Ann. Rev. Fluid Mech.*, vol. 8, 1976.
[141] L. F. Richardson, *Weather Prediction by Numerical Process*. Cambridge, UK: Cambridge Univ. Press, 1922.
[142] L. F. Richardson and J. A. Gaunt, *Diffusion Regarded as a Compensation for Smoothing*, Memoirs of the Roy. Meterolog. Soc., vol. 3, no. 30, pp. 171–175, 1930; reprinted in the collected papers of L. F. Richardson, vol. 1, Cambridge University Press, pp. 773–777, 1993.
[143] R. Robert, "Etat d'équilibre statistique pour l'écoulement bidimensionnel d'un fluide parfait," *C. R. Acad. Sc. Paris*, Série I, vol. 311, pp. 575–578, 1990.
[144] ——, "A maximum-entropy principle for two-dimensional perfect fluid dynamics," *J. Stat. Phys.*, vol. 65, pp. 531–553, 1991.
[145] R. Robert and J. Sommeria, "Statistical equilibrium states for two-dimensional flows," *J. Fluid Mech.*, vol. 229, pp. 291–310, 1991.
[146] A. Roshko, *J. Fluid Mech.*, vol. 10, p. 345, 1961.
[147] P. G. Saffman, "A note on the spectrum and decay of random two-dimensional vorticity distribution," *Stud. Appl. Math.*, vol. 50, pp. 377–383, 1971.
[148] J. Sommeria, C. Staquet, and R. Robert, "Final equilibrium state of a two-dimensional shear layer," *J. Fluid Mech.*, vol. 223, pp. 661–689, 1991.
[149] G. I. Taylor, "Diffusion by continuous movements," in *Proc. Lond. Math. Soc. Ser.*, no. 2, 1921, vol. 20, pp. 196–211.
[150] ——, "Statistical theory of turbulence," in *Proc. Roy. Soc. London A*, 1935, vol. 151, pp. 421–478.
[151] H. Tennekes and J. L. Lumley, *A First Course in Turbulence*. Cambridge, MA: MIT Press, 1972.
[152] A. A. Townsend, *The Structure of Turbulent Shear Flow*. Cambridge, UK: Cambridge Univ. Press, 1956.
[153] K. Urban, "A wavelet-galerkin algorithm for the driven-cavity-stokes-problem in two space dimensions," R.W.T.H. Aachen preprint, 1994.
[154] C. W. Van Atta and R. A. Antonia, "Reynolds dependence of sknewness and flatness factors of turbulent velocity derivatives," *Phys. Fluids*, vol. 23, pp. 252–257, 1980.
[155] J. C. Vassilicos, "The multi-spiral model of turbulence and intermittency," in *Topological Aspects of the Dynamics of Fluids and Plasmas*. Amsterdam: Kluwer, 1992, pp. 427–442.
[156] W. van der Water, "Experimental study of scaling in fully developed turbulence," *Turbulence in Spatially Extended Systems*, Benzi, Basdevant, and Ciliberto, Eds., pp. 189–213, 1993.
[157] M. Vergassola and U. Frisch, "Wavelet transforms of self-similar processes," *Physica D.*, 1991.
[158] J. Weiss, "The dynamics of enstrophy transfer in two-dimensional hydrodynamics," *Physica D.*, vol. 48, p. 273, 1992.
[159] M. V. Wickerhauser *et al.*, "Efficiency comparison of wavelet packet and adapted local cosine bases for compression of a two-dimensional turbulent flow," in *Wavelets: Theory, Algorithms and Applications*, Chui, Montefusco, and Puccio, Eds. New York: Academic, 1994, pp. 509–531.
[160] A. M. Yaglom, "Einstein's work on methods of processing fluctuating series of observations and the role of these methods in meteorology," *Izvestiya, Atmos. and Ocean. Phys.*, vol. 22, p. 1, 1986.
[161] V. Yakhot and S. A. Orszag, *Phys. Rev. Lett.*, vol. 57, p. 1722, 1986.
[162] V. Zimin, "Hierarchical model of turbulence," *Izvestiya, Atmos. and Ocean. Phys.*, vol. 17, pp. 941–949, 1981.
[163] ——, "Wavelet based model for small-scale turbulence," *Phys. Fluids*, vol. 7, no. 12, pp. 2925–2927, 1995.
[164] A. Zygmund, *Trigonometric Series*. New York: Cambridge, 1959.

Marie Farge received the M.S. degree from Stanford University, Stanford, CA, in 1977, the Ph.D. degree in physics from Université Paris VII in 1980, and the Ph.D. degree in mathematics from the Université Paris VI in 1987.

She is a Research Director at the Centre National à la Recherche Scientifique and is a member of the Laboratoire de Météorologie Dynamique, a CNRS laboratory which is connected to both the Ecole Normale Supérieure and the Ecole Polytechnique. She is presently researching the nonlinear dynamics of geophysical flows using computer simulation. In 1986 she pioneered the use of wavelets in fluid mechanics

Dr. Farge received several scientific prizes from CNRS, Cray Research, and French Academy of Science.

Nicholas Kevlahan received the B.Sc. degree (honors) in physics from the University of British Columbia, Vancouver, BC, Canada, in 1989, and in 1994 he received the Ph.D. degree for his work on structure and shocks in turbulence from the Department of Applied Mathematics and Theoretical Physics at the University of Cambridge, Cambridge, UK. He is now a postdoctoral Fellow at Laboratoire de Météorologie Dynamique du CNRS, Ecole Normale Supérieure, Paris. His research interests include the role of coherent structures in turbulence, wavelet analysis and simulation of turbulence, and the effects of straining on turbulent flows.

Valérie Perrier received the "agregation" in mathematics from the Ecole Normale Supérieure, St. Cloud, France, and the Ph.D. degree in mathematics from the Université Paris VI in 1991. She received the "habilitation" to conduct research in 1996.

She is an Assistant Professor of Mathematics at the Université Paris XIII. She is a numerical analyst and in 1989 introduced the use of wavelets to solve differential equations.

Éric Goirand is a Ph.D. student in mathematics at Université Paris VI. He received an engineering degree in computer science and a DEA (advanced studies degree) in signal processing.

He is presently working at ONERA, the French national laboratory for aeronautical research. He has used wavelet packets since 1991 and has written a parallel version of the the best basis algorithm of Victor Wickerhauser, with whom he worked for one year at Washington University in St. Louis, MO.

Mr. Goirand won the 1993 IBM prize for scientific computing.